Dynamic behavior of the circular membrane of an electrostatic microphone: Effect of holes in the backing electrode

Thomas Lavergne, Stéphane Durand,[a] Michel Bruneau, and Nicolas Joly
Laboratoire d'Acoustique de l'Université du Maine, UMR CNRS 6613, Université du Maine, Avenue Olivier Messiaen, 72 085 Le Mans Cedex 9, France

Dominique Rodrigues
Laboratoire National de métrologie et d'Essais (LNE), 29 Avenue Roger Hennequin, 78197 Trappes Cedex, France

(Received 16 May 2010; revised 2 September 2010; accepted 25 September 2010)

Today, several applications require using electrostatic microphones in environments and/or in frequency ranges, which are significantly different from those they were designed for. When low uncertainties on the behavior of acoustic fields, generated or measured by these transducers, are required, the displacement field of the diaphragm of the transducers (which can be highly nonuniform in the highest frequency range) must be characterized with an appropriate accuracy. An analytical approach, which leads to results depending on the location of the holes in the backing electrode (i.e., depending on the azimuthal coordinate) not available until now (regarding the displacement field of the membrane in the highest frequency range, up to 100 kHz), is presented here. The holes and the slit surrounding the electrode are considered as localized sources described by their volume velocity in the propagation equation governing the pressure field in the air gap (not by nonuniform boundary conditions on the surface of the backing electrode as usual). Experimental results, obtained from measurements of the displacement field of the membrane using a laser scanning vibrometer, are presented and compared to the theoretical results.
 [DOI: 10.1121/1.3504706]

PACS number(s): 43.38.Bs, 43.38.Kb [AJZ] Pages: 3459–3477

NOMENCLATURE

a	Radius of the membrane and radius of the backing electrode
c_0	Adiabatic speed of sound ($c_0 \cong 340$ m s^{-1} for air in standard conditions)
C_P	Heat coefficient at constant pressure per unit of mass of the gas
h_1	Length of the circular holes
h_2	Length of the peripheral slit
J_0 and J_1	Zero and one order Bessel functions of the first kind, respectively
j_{mn}	Zeros of the Bessel functions J_m, with $j_{00} = 2.40$, $j_{01} = 5.52$, $j_{02} = 8.65$, $j_{10} = 3.83$, $j_{11} = 7.015$, $j_{12} = 10.17$, $j_{20} = 5.13$, $j_{21} = 8.42$, $j_{22} = 11$, and so on
K_{mn}	Eigenvalues of the membrane subjected to Dirichlet condition at $r = a$
$k_v = [(1-i)/\sqrt{2}] \times \sqrt{\rho_0\omega/\mu}$	Wavenumber associated with the vortical movement due to viscosity effects (with a time factor given by $e^{i\omega t}$)
$k_h = [(1-i)/\sqrt{2}] \times \sqrt{\rho_0\omega C_P/\lambda_h}$	Wavenumber associated with the entropic movement due to heat conduction effects (with a time factor given by $e^{i\omega t}$)
$K = \omega\sqrt{M_S/T}$	Wavenumber of the membrane
M_S	Mass per unit area of the membrane
n_0	Number of holes in the backing electrode
O	Origin of the reference frame (set at the center of the membrane)
P_0	Static pressure
$p(r,\theta)$	The pressure field in the air gap between the membrane and the backing electrode
p_{av}	Driving harmonic acoustic pressure wave (assumed to be uniform over the surface of the membrane)
p_C	Pressure variation in the backchamber
r	Radial coordinate
r_1	Distance between the center of the circular backing electrode and the center of any hole
r_2	Distance between the center of the circular backing electrode and the peripheral slit ($r_2 \cong a$)
R	Radius of the circular holes
S_b	Total area of the backing electrode
S_{1,v_0}	Area of a hole
$S_1 = \sum_{v_0=1}^{n_0} S_{1,v_0}$	Total area of the holes
S_2	Area of the peripheral slit
T	Tension of the membrane
U_{1,v_0}	Volume velocity of each hole (positive when directed along the z-axis)

[a]Author to whom correspondence should be addressed. Electronic mail: Stephane.Durand@univ-lemans.fr

$U_1 = \sum_{v_0=1}^{n_0} U_{1,v_0}$ Total volume velocity of the holes (positive when directed along the z-axis)

$U(\theta)$ Volume velocity of the peripheral slit per unit angle (positive when directed along the z-axis)

U_2 Total volume velocity of the peripheral slit (positive when directed along the z-axis)

v_r Radial particle velocity in the fluid gap

$Y_C = -[U_1 + U_2]/p_C$ Input admittance of the backchamber (when considered as a small cavity of volume V_C behind the backing electrode), ratio of the input volume velocity and the pressure variation

y_{1,v_0} Transfer admittance of hole numbered v_0

y Local transfer admittance of the slit

z Coordinate normal to the membrane and the backing electrode (Oz being outwardly directed through the membrane)

Z_{av} Input impedance of the microphone

Z_C Input impedance of the small cavity of volume V_C

$Z_m = L_m + \frac{1}{i\omega C_m}$ Mechanical impedance of the membrane

$Z_\mu = R_\mu + i\omega L_\mu$ Mechanical impedance of the air gap

$Z_h = R_h + \frac{1}{i\omega C_h}$ Thermal impedance of the air gap

Z_1 Total input impedance of the holes

Z_2 Input impedance of the slit

Greek symbols

$\hat{\beta} = (\partial_T P)_V$ Increase in pressure per unit increase in temperature at constant volume

γ Specific heat ratio

γ_{mn} Zeros of the first derivative of the Bessel functions J_m, with $\gamma_{00} = 0$, $\gamma_{01} = 3.83$, $\gamma_{02} = 7.02$, $\gamma_{10} = 1.84$, $\gamma_{11} = 5.33$, $\gamma_{12} = 8.54$, $\gamma_{20} = 3.05$, $\gamma_{21} = 6.71$, $\gamma_{22} = 9.97$, and so on

ε Thickness of the fluid film trapped between the membrane and the backing electrode

ε_C Thickness of the backchamber

θ Azimuthal coordinate ($\theta = 0$ at the center of a hole in the backing electrode)

θ_{v_0} Azimuthal coordinate of the v_0th hole, $v_0 = 1, \ldots, n_0$

λ_h Coefficient of thermal conductivity of the gas [$\lambda_h/(\rho_0 c_0 C_P) \cong 5.8 \times 10^{-8}$ m for air in standard conditions]

κ_{mn} Eigenvalues of the fluid film subjected to Neumann condition at $r = a$

μ Shear viscosity coefficient of the gas ($\mu \cong 1.9 \times 10^{-5}$ kg m^{-1} s^{-1} for air in standard conditions)

$\xi(r, \theta)$ Displacement field of the membrane (positive when directed along the z-axis)

ρ_0 Density of the gas ($\rho_0 \cong 1.2$ kg m^{-3} for air in standard conditions)

σ Sensitivity of the microphone

τ Temperature variation in the air gap

$\phi_r = S_1/S_b$ Ratio of the total area of the holes to the total backing electrode area

$\varphi_{mn}(r, \theta)$ Eigenfunctions of the fluid film subjected to Neumann condition at $r = a$

$\chi_T \approx 1/P_0$ Isothermal compressibility of air

$\psi_{mn}^{(s)}(r, \theta)$ Eigenfunctions of the membrane subjected to Dirichlet condition at $r = a$

ω Angular frequency

Notation

$\langle f_1(r, \theta) | f_2(r, \theta) \rangle$ $\iint_S f_1 f_2 \, dS = \int_0^{2\pi} \int_0^a f_1 f_2 \, r \, dr \, d\theta$ inner product (domain of area $S = \pi a^2$)

$\langle f(r, \theta) \rangle$ $\int_0^{2\pi} \int_0^a f(r, \theta) \, r \, dr \, d\theta$

$\langle f_1(r) | f_2(r) \rangle$ $\int_0^a f_1 f_2 \, r \, dr$

$\langle f(r) \rangle$ $\int_0^a f(r) \, r \, dr$

I. INTRODUCTION

Numerous works on the measurement condenser microphones, used as either emitters or receivers, have been carried out for more than half a century (see Refs. 1–14). More specifically the works presented in Ref. 7, further emphasized in Ref. 8, enable a description of the effects of the holes (including their location in the backing electrode) on the microphone performances (sensitivity, bandwidth, and mechanical-thermal noise). During the past decades, few works have examined the influence of static pressure, static temperature, and gas composition on the behavior of these microphones,[15–17] which were motivated by a quite recent rising demand. Today, several applications require using such transducers in environments and/or in frequency ranges which are significantly different from those for which they were designed. The primary calibration of the condenser microphones in the highest frequency range[18,19] and the determination of the Boltzmann constant by an acoustic method over a wide static pressure range and over a wide frequency range,[20] are examples of such applications.

Actually, these applications, among others, are greatly in need of an accurate characterization of the transducers in unusual situations. More particularly, when low uncertainties on the behavior of acoustic fields, generated or measured by the transducers, are required close to the transducers and/or in closed small cavities or resonators, the displacement field of the diaphragm of the transducers (which can be highly nonuniform, especially in the highest frequency range) and the coupling factor between the transducer and the acoustic field must be modeled with an appropriate accuracy.

Most of the analytical works on the behavior of the electrostatic microphones mentioned above deal primarily, among others, with (i) the description of the input impedance (or the sensitivity) through the behavior of an adapted lumped element circuit,[11] (ii) the global description (i.e., spatially averaged over the surface of the transducer) of the coupling

between the membrane, and both the fluid gap (trapped between the membrane and the backing electrode) and the backchamber (through the holes set in the backing electrode and the slit surrounding it),[5–7] (iii) the modeling of the dissipative effects of the holes,[4,9,10] and (iv) the modeling of the effect of specific shapes of the backing electrode.[13,14] In all cases, the theoretical behavior of the pressure variations is investigated in the fluid gap, in the holes (when existing) and in the peripheral slit, and in the backchamber, the coupling with the membrane being accounted for. But, despite these advances in the modeling of condenser microphones, today the analytical procedure whereby the effects of the location of the holes are not averaged over the surface of the backing electrode but are accounted for in both the displacement field and the pressure variations, leading to results which depend not only on the radial coordinate but also on the azimuthal coordinate, provides situations not considered so far, to our knowledge, for describing the behavior of the membrane up to 100 kHz (the location of the holes is playing an important role). Thus, the aim of the paper is twofold: (i) To provide such new modeling using a method relying on the sets of the appropriate eigenmodes of both the membrane and the pressure fields behind the membrane and relying on the Green's theorem and the associated integral formulation for part of the solution and (ii) to compare the theoretical results obtained on the displacement field of the membrane to the experimental results obtained from measurements using a laser scanning vibrometer.[21,22]

In the present modeling, the effects of the z-components (perpendicular to the membrane) of the volume velocities of the holes and the slit on the particle velocity inside the air gap are not taken into account by appropriate boundary conditions on the surface of the backing electrode as usual because these boundary conditions depend strongly on both the coordinates r and θ. Such boundary conditions would prevent us from obtaining an analytical solution, except when averaging on the surface of the backing electrode (but therefore the solution would not depend on the azimuthal coordinate as mentioned before).[5–7,21,22] It is the reason why the holes and the slit are considered as local sources described by the axial component of the volume velocity in the right hand side of the propagation equation. Moreover, the presence of the holes is also taken into account by an averaged slip condition and an averaged polytropic thermal condition (both depending on the ratio of the total area of the holes to the total backing electrode area S_b) through the wavenumber associated to the pressure variation in the fluid gap. The theoretical results obtained from this analytical approach, which leads to results depending on the location of the holes in the backing electrode (i.e., depending on the azimuthal coordinate), are presented and compared to the experimental results obtained from measurements of the displacement field of the membrane using a laser scanning vibrometer.

II. THE FUNDAMENTAL PROBLEM

The cylindrical coordinate system used (r,θ,z) has its origin at the center O of the membrane, and the Oz-axis is perpendicular to the membrane and outwardly directed as indicated in Fig. 1. The holes in the backing electrode are

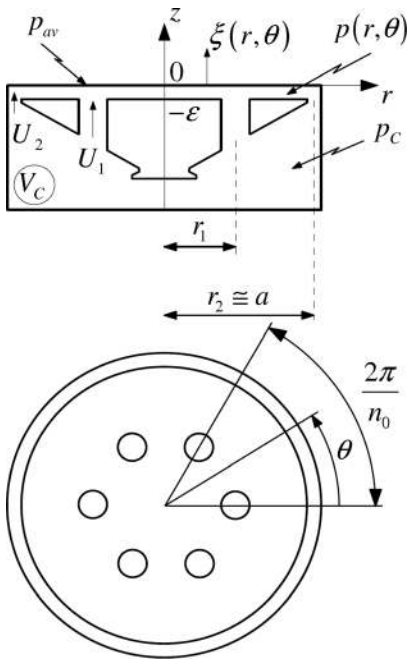

FIG. 1. Electrostatic microphones showing the membrane, the backing electrode with holes regularly azimuthally distributed, the peripheral slit, and the backchamber.

regularly azimuthally distributed at the distance r_1 from the center. The origin $(\theta = 0)$ of the azimuthal coordinate θ is set at the center of a hole in the backing electrode. The thickness of the fluid film trapped between the membrane and the backing electrode is denoted ε (the coordinate of the upper surface of the backing electrode is "$-\varepsilon$"). It has the same order of magnitude as the thickness of the viscous and thermal boundary layers. The pressure variation is assumed to be constant through the thickness of the fluid gap between the membrane and the backing electrode (it does not depend on the z-coordinate). Note that, in the lower frequency range, the backchamber would behave as a small cavity because the depth of this backing cavity is very small (and nonuniform) and because the outputs of the slit and the holes are quite evenly distributed on the interface between this backchamber and the backing electrode (this point is discussed below in Sec. III C).

A. Equations governing the displacement field of the membrane

The set of equations which govern the displacement field $\xi(r,\theta)$ of the membrane (positive when directed along the z-axis), supported on a rigid circular frame at its periphery $r = a$ (Dirichlet boundary condition), driven by a harmonic acoustic pressure p_{av} assumed to be uniform over the surface of the membrane, and loaded by the pressure field $p(r,\theta)$ in the air gap between the membrane and the backing electrode, can be written as

$$T\left(\partial_{rr}^2 + \frac{1}{r}\partial_r + \frac{1}{r^2}\partial_{\theta\theta}^2 + K^2\right)\xi(r,\theta) = p_{av} - p(r,\theta), \tag{1a}$$

$$\xi(r = a,\theta) = 0, \tag{1b}$$

where $K = \omega\sqrt{M_S/T}$, with T and M_S being, respectively, the tension of the membrane and its mass per unit area, and ω is the angular frequency.

B. Equations governing the pressure variations in the air gap

The no-slip condition requires the radial velocity v_r in the fluid gap to vanish on the membrane ($v_r = 0$) because this radial velocity is assumed here to be much greater than the azimuthal velocity v_θ. This is approximately valid on the backing electrode with sparse holes array, due to the no-slip condition everywhere, but not at the locations of the holes where the radial velocity v_r should approximately be given by Euler equation

$$v_r \cong \left[\frac{-1}{(i\omega\rho_0)}\right]\partial_r p. \tag{2a}$$

Therefore, an accurate homogeneous boundary condition would allow for slight slip condition at the backing electrode to account for the presence of the holes, namely

$$v_r \cong \left[\frac{-\phi_r}{(i\omega\rho_0)}\right]\partial_r p. \tag{2b}$$

As a first approach, neglecting here the spatial orientation of the holes (i.e., v_r and p do not depend on the azimuthal angle θ here), the parameter ϕ_r can be assumed to be a constant equal to the ratio of the total area of the holes to the total backing electrode area S_b,

$$\phi_r = \frac{1}{S_b}\left(\sum_{v_0=1}^{n_0} S_{1,v_0}\right). \tag{2c}$$

Therefore, the usual solution (when $\phi_r = 0$, no hole) for the mean value $\bar{v}_r$ of the radial velocity v_r across the thickness of the air gap, namely (see Ref. 23, Chap. 3 and Appendix C),

$$\bar{v}_r = \left[\frac{-F_v^0}{(i\rho_0\omega)}\right]\partial_r p \tag{3a}$$

with

$$F_v^0 = 1 - \frac{\tan(k_v\varepsilon/2)}{k_v\varepsilon/2}, \tag{3b}$$

takes the following form, when the area ratio ϕ_r does not vanish[11] (details are given in Appendix C):

$$\bar{v}_r = \left[\frac{-F_v}{(i\rho_0\omega)}\right]\partial_r p, \tag{4a}$$

where

$$F_v = 1 - \frac{2-\phi_r}{2}\frac{\tan(k_v\varepsilon/2)}{k_v\varepsilon/2}, \tag{4b}$$

$k_v = \left[(1-i)/\sqrt{2}\right]\sqrt{\rho_0\omega/\mu}$ being the wavenumber associated with the vortical movement due to viscosity effects (with a time factor given by $e^{i\omega t}$), ρ_0 and μ being, respectively, the density and the shear viscosity coefficient of the gas.

The isothermal condition requires the temperature variation τ in the fluid gap to vanish on the membrane ($\tau = 0$). Similarly to the radial velocity, this is approximately valid, on the backing electrode with sparse holes array, due to the isothermal condition everywhere but not at the locations of the holes where the temperature variation τ should correspond to a thermodynamic process which would be quasi-adiabatic. Therefore, accounting for the presence of the holes in the same way as the one mentioned above (when the area ratio ϕ_r does not vanish), the solution for the mean value $\bar{\tau}$ of the temperature variation τ across the thickness of the air gap takes the following form (see Ref. 23, Chap. 3, and Appendix C):

$$\bar{\tau} = F_h\frac{\gamma-1}{\hat{\beta}\gamma}p, \tag{5a}$$

where $\hat{\beta} = (\partial_T P)_V$ is the increase in pressure per unit increase in temperature at constant volume, γ the specific heat ratio, and where

$$F_h = 1 - \frac{2-\phi_r}{2}\frac{\tan(k_h\varepsilon/2)}{k_h\varepsilon/2}, \tag{5b}$$

$k_h = \left[(1-i)/\sqrt{2}\right]\sqrt{\rho_0\omega C_P/\lambda_h}$ being the wavenumber associated with the entropic movement due to conduction effects (with a time factor given by $e^{i\omega t}$), C_P and λ_h being, respectively, the heat coefficient at constant pressure per unit of mass and the coefficient of thermal conductivity of the gas.

Moreover, assuming that each hole and the peripheral slit behave as localized sources (more exactly as localized sinks) described by the z-component of their volume velocity (positive when directed along the z-axis), respectively, U_{1,v_0} (for each hole labeled v_0) and U_2 (for the slit), and assuming Neumann boundary condition on the external side of the fluid layer (i.e., at $r \cong a$), the set of equations which govern the pressure field $p(r, \theta)$ inside the air gap is given by[23]

$$\left(\partial_{rr}^2 + \frac{1}{r}\partial_r + \frac{1}{r^2}\partial_{\theta\theta}^2 + \chi^2\right)p(r,\theta) = -\frac{\rho_0\omega^2}{F_v}\frac{\xi(r,\theta)}{\varepsilon} - \frac{i\omega\rho_0}{F_v}\left[\sum_{v_0=1}^{n_0}\frac{U_{1,v_0}(r,\theta)}{\varepsilon}\frac{\delta(r-r_1)}{r}\times\delta(\theta-\theta_{v_0}) + \frac{U(\theta)}{\varepsilon}\frac{\delta(r-r_2)}{r}\right], \tag{6a}$$

$$\partial_r p(r=a,\theta) = 0, \tag{6b}$$

where the complex wavenumber χ accounts for the angular frequency ω of the field and the properties of the fluid, namely the compressibility and the density ρ_0 through the adiabatic speed of sound c_0, the heat capacity at constant pressure per unit of mass C_p, the specific heat ratio γ, the

shear viscosity coefficient μ, and the thermal conduction coefficient λ_h,

$$\chi^2 = \frac{\omega^2}{c_0^2}\frac{1+(\gamma-1)(1-F_h)}{F_v}, \tag{6c}$$

and where $\delta(r-r_i)$ and $\delta(\theta-\theta_{v_0})$ are Dirac functions, r_1 and r_2 being the distance between the center of the circular backing electrode and, respectively, the center of any hole and the peripheral slit. Note that the total volume velocity of the n_0 holes U_1 and the peripheral slit U_2 in the fluid gap can be expressed, respectively, in the following manner:

$$U_1 = \int_0^a r\,dr \int_0^{2\pi} d\theta \int_{-\varepsilon}^0 dz \times \sum_{v_0=1}^{n_0} \frac{U_{1,v_0}(r,\theta)}{\varepsilon}\,\frac{\delta(r-r_1)}{r}\,\delta(\theta-\theta_{v_0}), \tag{6d}$$

$$U_2 = \int_0^{2\pi} U(\theta)\,d\theta = \int_0^a r\,dr \int_0^{2\pi} d\theta \int_{-\varepsilon}^0 dz\,\frac{U(\theta)}{\varepsilon}\,\frac{\delta(r-r_2)}{r}. \tag{6e}$$

It is worth noting that, here, the effect of the z-components of the volume velocities of the holes and the slit on the particle velocity inside the air gap are not taken into account by appropriate boundary conditions on the surface of the backing electrode because these boundary conditions depend strongly on both coordinates r and θ. Such boundary conditions would prevent us from obtaining an analytical solution, except when averaging on the surface of the backing electrode (but, therefore, the solution would not depend on the azimuthal coordinate θ).[5–7] It is the reason why the holes and the slit are considered as local sources (described by the z-component of the volume velocity) in the right hand side of the propagation equation (the pressure p is assumed to be independent of the coordinate z). Moreover, the presence of the holes is also taken into account by a nonvanishing radial component of the particle velocity and a nonisothermal condition on the surface of the backing electrode (as presented above). These effects are expressed by an averaged slip condition and an averaged polytropic thermal condition (both depending on the area ratio ϕ_r), through the functions F_v and F_h in the wavenumber χ (taking these averages is sufficient here because their influence on the θ-component of the displacement field of the membrane would be negligible).

C. Coupling between the pressure field in the air gap and the pressure field inside the backchamber

The aim of the present work is to show the local influence of holes in the backing electrode on the displacement field of the membrane, an appropriate modeling of both the input admittance of the backchamber (which depends on the location) and the input admittance of each hole y_{1,v_0} and the slit y is needed.

It is worth noting that, in the highest frequency range, the backchamber cannot be considered as a small cavity: A modal field takes place. In the present situation (regular azimuthal distribution of the holes), the acoustic pressure field $p_C(r,\theta)$ in the backchamber is assumed to depend on both the radial coordinate r and the azimuthal coordinate θ. Thus, it is assumed to be the solution of the propagation equation, which presents the same form as Eq. (6a),

$$\left(\partial_{rr}^2 + \frac{1}{r}\partial_r + \frac{1}{r^2}\partial_{\theta\theta}^2 + \chi_C^2\right) p_C(r,\theta) = \frac{i\omega\rho_0}{F_{vC}}\left[\sum_{v_0=1}^{n_0}\frac{U_{1,v_0}(r,\theta)}{\varepsilon_C}\,\frac{\delta(r-r_1)}{r}\,\delta(\theta-\theta_{v_0}) + \frac{U(\theta)}{\varepsilon_C}\,\frac{\delta(r-r_2)}{r}\right], \tag{7}$$

and to be subjected to Neumann boundary conditions at the periphery ($r=a$), ε_C, $p_C(r,\theta)$, and χ_C being, respectively, the mean thickness of the cavity (given by the ratio of its volume to its surface), the pressure variation, and the complex wavenumber given by Eq. (6c), where the thickness ε, which appears in expressions (4b) and (5b) of the functions F_v and F_h (denoted here, respectively, F_{vC} and F_{hC}), is replaced by the thickness ε_C.

On the other hand, the dimensions of the holes and the slit are such that they do not behave as capillary tubes or a slit[24] because the present modeling is dedicated to the highest frequency range (typically up to 100 kHz). Assuming plane wave approximation in each hole (cylindrical tube of area S_{1,v_0}) for the pressure variation and assuming that the thickness of the viscous boundary layer is much lower than the radius R of the hole (the effect of the thermal boundary layer is neglected in the backchamber), the pressure difference between the ends of a hole is given by the Poiseuille law averaged across the section of the hole, which takes the following form when the length h_1 of the tube is much lower than the wavelength (i.e., the volume velocity is assumed to be independent of the coordinate z inside the holes):[23]

$$U_{1,v_0} = y_{1,v_0}\,[p_C(r_1,0) - p_1], \tag{8a}$$

with $p_1 = p(r_1,\,\theta=0)$ (each hole playing the same role in the modeling) and where the admittance y_{1,v_0} is given by

$$y_{1,v_0} = \frac{S_{1,v_0}(1-K_v)}{i\omega\rho_0 h_1}, \tag{8b}$$

with

$$K_v = \frac{2}{k_v R}\frac{J_1(k_v R)}{J_0(k_v R)}, \tag{8c}$$

J_0 and J_1 being, respectively, the zero and one order Bessel functions of the first kind.

Assuming that the holes behave in the same manner, the total volume velocity of the holes

$$U_1 = \sum_{v_0=1}^{n_0} U_{1,v_0} = n_0 U_{1,v_0} \tag{9a}$$

is then associated with the total admittance

$$Y_1 = \frac{1}{Z_1} = n_0 y_{1,v_0} \tag{9b}$$

by the relation

$$U_1 = Y_1[p_C(r_1,0) - p_1]. \tag{9c}$$

In the same manner, the volume velocity per unit angle $U(\theta)$ (along the z-axis) at the input of the peripheral slit (the interface between the slit and the air gap) can be written as

$$U(\theta) = y[p_C(r_2,\theta) - p(r_2,\theta)], \tag{10a}$$

where y is the input admittance of the peripheral slit given by

$$y = \frac{s_2(1-\Gamma_v)}{i\omega\rho_0 h_2}, \tag{10b}$$

with

$$\Gamma_v = \frac{1}{k_v e/2}\tan(k_v e/2), \tag{10c}$$

$$s_2 = \frac{S_2}{(2\pi)} = ae, \tag{10d}$$

e denoting the width of the slit.

When assuming that the length h_2 of the slit is very small (compared with its width e), Eq. (10a) can be replaced by the continuity condition

$$p(r_2,\theta) = p_C(r_2,\theta). \tag{10e}$$

III. COUPLED SOLUTIONS FOR THE DISPLACEMENT FIELD OF THE MEMBRANE AND THE PRESSURE VARIATION IN THE AIR GAP AND THE BACKCHAMBER

A. Solution for the displacement field of the membrane

The solution for the displacement field of the membrane [Eqs. (1a) and (1b)] can be expressed as the sum of three functions as follows:

$$\xi(r,\theta) = \frac{p_{av}}{TK^2}\left[1 - \frac{J_0(Kr)}{J_0(Ka)}\right] + \sum_{mn\sigma}\Xi_{mn}^{(\sigma)}\psi_{mn}^{(\sigma)}(r,\theta), \tag{11a}$$

where the first one $p_{av}/(TK^2)$ is the solution of the equation of the membrane when the movement is forced by the uniform (over the surface of the membrane) harmonic pressure field p_{av} (p_{av} being applied on the outer side of the membrane), the second one is the general solution $J_0(Kr)$ (zero order Bessel function of the first kind) of the homogeneous equation of the membrane (the sum of the first two terms being subjected to the Dirichlet boundary condition), and the third one is given by an expansion on the orthonormal eigenfunctions $\psi_{mn}^{(\sigma)}(r,\theta)$ (twice degenerated, with associated eigenvalues K_{mn}) of the membrane supported on a rigid frame at its periphery $r = a$ (Dirichlet condition) *in vacuo*, the right hand side of the Eq. (11a) being given by the pressure variation in the air gap $p(r,\theta)$, leading to

$$\Xi_{mn}^{(\sigma)} = \frac{\langle p(r,\theta)|\psi_{mn}^{(\sigma)}(r,\theta)\rangle}{T\left(K_{mn}^2 - K^2\right)}, \tag{11b}$$

the inner product over the surface of the membrane S_M, represented by the bracket $\langle f_1, f_2\rangle = \iint_{S_M} f_1 f_2\, dS_M$, showing the coupling effect with the pressure variation $p(r,\theta)$ inside the air gap.

The eigenfunctions $\psi_{mn}^{(\sigma)}(r,\theta)$ and their associated eigenvalues K_{mn} are given by

$$\psi_{mn}^{(1)}(r,\theta) = N_{mn}J_m(K_{mn}r)\cos(m\theta), \tag{12a}$$

$$\psi_{mn}^{(2)}(r,\theta) = N_{mn}J_m(K_{mn}r)\sin(m\theta), \tag{12b}$$

with, respectively, for $m = 0$ and $m \neq 0$,

$$N_{0n}^{-1} = \sqrt{\pi}\, aJ_1(K_{0n}a), \tag{12c}$$

$$N_{mn}^{-1} = \sqrt{\pi/2}\, aJ_{m-1}(K_{mn}a), \tag{12d}$$

where $K_{mn}a = j_{mn}$ are the zeros of the Bessel functions J_m.

It is worth noting that the first part of the solution (11a), which satisfies the Dirichlet conditions at $r = a$, is expressed below as an expansion on the eigenfunctions $\psi_{mn}^{(\sigma)}(r,\theta)$,

$$\sum_{mn\sigma}\zeta_{mn}^{(\sigma)}\psi_{mn}^{(\sigma)}(r,\theta), \tag{13a}$$

with

$$\zeta_{mn}^{(\sigma)} = \frac{p_{av}}{TK^2}\left\langle\left[\frac{1 - J_0(Kr)}{J_0(Ka)}\right]\middle|\psi_{mn}^{(\sigma)}\right\rangle. \tag{13b}$$

Then, the solution for the displacement field of the membrane can take the following form:

$$\xi(r,\ \theta) = \sum_{mn\sigma}\xi_{mn}^{(\sigma)}\psi_{mn}^{(\sigma)}(r,\theta), \tag{14a}$$

where

$$\xi_{mn}^{(\sigma)} = \zeta_{mn}^{(\sigma)} + \Xi_{mn}^{(\sigma)} = \frac{p_{av}}{TK^2}\left\langle\left[1 - \frac{J_0(Kr)}{J_0(Ka)}\right]\middle|\psi_{mn}^{(\sigma)}(r,\theta)\right\rangle + \frac{\langle p(r,\theta)|\psi_{mn}^{(\sigma)}(r,\theta)\rangle}{T\left(K_{mn}^2 - K^2\right)}. \tag{14b}$$

According to the orthogonality properties of the trigonometric functions, Eq. (14b) takes the following form:

$$\xi_{mn}^{(\sigma)} = \zeta_{mn}^{(\sigma)} + \Xi_{mn}^{(\sigma)} = \frac{p_{av}}{TK^2}N_{0n}\left[\frac{a}{K_{0n}}J_1(K_{0n}a) - \frac{aK_{0n}J_0'(K_{0n}a)}{K^2 - K_{0n}^2}\right]\delta_{\mu 0}\delta_{\sigma 1} + \frac{\langle p(r,\theta)|\psi_{mn}^{(\sigma)}(r,\theta)\rangle}{T\left(K_{mn}^2 - K^2\right)}. \tag{14c}$$

It is worth noting that the solution for the displacement field can be directly expressed as given by Eq. (14a), with

$$\xi_{mn}^{(\sigma)} = \frac{\langle p(r,\theta) - p_{av} | \psi_{mn}^{(\sigma)}(r,\theta) \rangle}{T\left(K_{mn}^2 - K^2\right)}. \tag{15}$$

B. Solution for the pressure variation in the air gap

The pressure variation $p(r,\theta)$ solution of the propagation Eq. (6a) subjected to the Neumann boundary condition (6b) is written as the following sum:

$$p(r,\theta) = p_h(r,\theta) + p_\xi(r,\theta) + p_u(r,\theta), \tag{16a}$$

where

$$\left(\partial_{rr}^2 + \frac{1}{r}\partial_r + \frac{1}{r^2}\partial_{\theta\theta}^2 + \chi^2\right) p_h(r,\theta) = 0, \tag{16b}$$

$$\left(\partial_{rr}^2 + \frac{1}{r}\partial_r + \frac{1}{r^2}\partial_{\theta\theta}^2 + \chi^2\right) p_\xi(r,\theta) = -\rho_0\omega^2 \frac{\xi(r,\theta)}{\varepsilon F_v}, \tag{16c}$$

$$\left(\partial_{rr}^2 + \frac{1}{r}\partial_r + \frac{1}{r^2}\partial_{\theta\theta}^2 + \chi^2\right) p_u(r,\theta) = -\frac{i\omega\rho_0}{F_v}\left[\sum_{v_0=1}^{n_0} \frac{U_{1,v_0}(r,\theta)}{\varepsilon}\frac{\delta(r-r_1)}{r}\delta(\theta-\theta_{v_0}) + \frac{U(\theta)}{\varepsilon}\frac{\delta(r-r_2)}{r}\right]. \tag{16d}$$

The solution of Eq. (16b) is given by

$$p_h(r,\theta) = \sum_m \left[A_m^{(1)}\cos(m\theta) + A_m^{(2)}\sin(m\theta)\right] J_m(\chi r), \tag{17}$$

where the coefficients $A_m^{(\sigma)}$ are integration constants.

The solution of Eq. (16c) can be expressed as an expansion of the Dirichlet eigenfunctions of the membrane, namely

$$p_\xi(r,\theta) = \sum_{mn\sigma} p_{\xi mn}^{(\sigma)} \psi_{mn}^{(\sigma)}(r,\theta), \tag{18a}$$

with

$$p_{\xi mn}^{(\sigma)} = \frac{\rho_0\omega^2}{\varepsilon F_v}\frac{\xi_{mn}^{(\sigma)}}{K_{mn}^2 - \chi^2}, \tag{18b}$$

where the expressions of the eigenfunctions $\psi_{mn}^{(\sigma)}(r,\theta)$ and the values of the eigenvalues K_{mn} are given in Eqs. (12a)–(12d).

Neither p_h nor p_ξ satisfies the Neumann boundary condition at $r = a$, but their sum is subjected to this condition (6b). This implies that in using the orthogonality property of the trigonometric functions $\cos(m\theta)$ and $\sin(m\theta)$ and invoking Eq. (18b),

$$A_m^{(\sigma)} = -\sum_n \frac{p_{\xi mn}^{(\sigma)} N_{mn}\,\partial_r J_m(K_{mn}a)}{\partial_r J_m(\chi a)} = -\frac{1}{\chi J_m'(\chi a)}\sum_n \frac{\rho_0\omega^2}{\varepsilon F_v}\frac{\xi_{mn}^{(\sigma)} N_{mn}}{K_{mn}^2 - \chi^2} K_{mn} J_m'(K_{mn}a). \tag{18c}$$

Finally, the solution of Eq. (16d) can be written as

$$p_u(r,\theta) = \frac{i\omega\rho_0}{F_v}\iint G(r,\theta;r_0,\theta_0) \times \left[\sum_{v_0=1}^{n_0}\frac{U_{1,v_0}(r_0,\theta_0)}{\varepsilon}\frac{\delta(r_0-r_1)}{r_0}\delta(\theta_0-\theta_{v_0}) + \frac{U(\theta_0)}{\varepsilon}\frac{\delta(r_0-r_2)}{r_0}\right] r_0\,dr_0\,d\theta_0, \tag{19a}$$

where the volume velocities $U_1 = \sum_{v_0=1}^{n_0} U_{1,v_0}$ and $U(\theta_0)$ are given by solving the set of Eqs. (7)–(10), which govern the coupling between the pressure field in the air gap and the pressure field inside the backchamber (see next Sec. III C), and where the Green's function, which is assumed to satisfy Neumann boundary conditions, can be expressed as an expansion on orthonormal Neumann eigenfunctions $\varphi_{mn}^{(\sigma)}(r,\theta)$ (with associated eigenvalues κ_{mn}),

$$G(r,\theta;r_0,\theta_0) = \sum_{mn\sigma}\frac{\varphi_{mn}^{(\sigma)}(r_0,\theta_0)}{\kappa_{mn}^2 - \chi^2}\varphi_{mn}^{(\sigma)}(r,\theta). \tag{19b}$$

The eigenfunctions $\varphi_{mn}^{(\sigma)}(r,\theta)$and their associated eigenvalues κ_{mn} are given by

$$\varphi_{mn}^{(1)}(r,\theta) = v_{mn} J_m(\kappa_{mn}r)\cos(m\theta), \tag{20a}$$

$$\varphi_{mn}^{(2)}(r,\theta) = v_{mn} J_m(\kappa_{mn}r)\sin(m\theta), \tag{20b}$$

where $\kappa_{mn}a = \gamma_{mn}$ are the zeros of the first derivative of the Bessel functions J_m, with

$$v_{mn}^{-1} = \frac{a}{\sqrt{2}}\sqrt{(1+\delta_{m0})\pi}\sqrt{1-(m/\gamma_{mn})^2}\,J_m(\gamma_{mn}) \quad \text{if } \gamma_{mn} \neq 0, \tag{20c}$$

$$v_{mn}^{-1} = \frac{a}{\sqrt{2}}\sqrt{(1+\delta_{m0})\pi} \quad \text{if } \gamma_{mn} = 0, \tag{20d}$$

δ_{m0} being the Kronecker index, $m, n \geq 0$ (integers).

Finally, solution (19a) takes the following form:

$$p_u(r,\theta) = \frac{i\omega\rho_0}{F_v}\sum_{mn}\frac{v_{mn}^2 J_m(\kappa_{mn}r)}{\kappa_{mn}^2 - \chi^2} \times \left\{\left[\sum_{v_0=1}^{n_0}\frac{U_{1,v_0}(r_1,\theta_{v0})}{\varepsilon}J_m(\kappa_{mn}r_1)\cos(m\theta_{v_0}) + \frac{1}{\varepsilon}J_m(\kappa_{mn}r_2)\langle U(\theta_0)|\cos(m\theta_0)\rangle\right]\cos(m\theta) + \left[\sum_{v_0=1}^{n_0}\frac{U_{1,v_0}(r_1,\theta_{v0})}{\varepsilon}J_m(\kappa_{mn}r_1)\sin(m\theta_{v_0}) + \frac{1}{\varepsilon}J_m(\kappa_{mn}r_2)\langle U(\theta_0)|\sin(m\theta_0)\rangle\right]\sin(m\theta)\right\}, \tag{21}$$

where $\langle f_1(\theta_0)|f_2(\theta_0)\rangle = \int_0^{2\pi} f_1(\theta_0)f_2(\theta_0)\,d\theta_0$.

Using the following notations for the unknown quantities

$$V_m^{(1)} = \sum_{v_0=1}^{n_0} U_{1,v_0}(r_1,\theta_{v0})\cos(m\theta_{v_0}),$$
$$V_m^{(2)} = \sum_{v_0=1}^{n_0} U_{1,v_0}(r_1,\theta_{v0})\sin(m\theta_{v_0}), \tag{22a}$$

$$U_m^{(1)} = \langle U(\theta_0)|\cos(m\theta_0)\rangle,$$
$$U_m^{(2)} = \langle U(\theta_0)|\sin(m\theta_0)\rangle, \tag{22b}$$

with $r_2 \cong a$,

Eq. (21) becomes

$$p_u(r,\theta) = \frac{i\omega\rho_0}{\varepsilon F_v}\sum_{mn}\frac{v_{mn}^2 J_m(\kappa_{mn}r)}{\kappa_{mn}^2-\chi^2} \times\left\{\left[V_m^{(1)}J_m(\kappa_{mn}r_1)+U_m^{(1)}J_m(\kappa_{mn}r_2)\right]\cos(m\theta) + \left[V_m^{(2)}J_m(\kappa_{mn}r_1)+U_m^{(2)}J_m(\kappa_{mn}r_2)\right]\sin(m\theta)\right\}. \tag{23}$$

It is worth noting that, owing to the origin of the azimuthal angle θ at the center of a hole and the symmetry of the problem, it is assumed that $\cos(m\theta_{v_0}) = 1$ and $\sin(m\theta_{v_0}) = 0$ (i.e., $m = 0, n_0, 2n_0, 3n_0, \ldots, n_0$ being the number of holes). Therefore, invoking expressions (9a) of the total volume velocity of the holes U_1, Eq. (22a) becomes:

$$V_m^{(1)} = U_1,$$
$$V_m^{(2)} = 0, \tag{24a}$$

leading to

$$p_u(r,\theta) = \frac{i\omega\rho_0}{\varepsilon F_v}\sum_{mn}\frac{v_{mn}^2 J_m(\kappa_{mn}r)}{\kappa_{mn}^2-\chi^2} \times\left\{\left[U_1 J_m(\kappa_{mn}r_1)+U_m^{(1)}J_m(\kappa_{mn}r_2)\right]\cos(m\theta) + U_m^{(2)}J_m(\kappa_{mn}r_2)\sin(m\theta)\right\}. \tag{24b}$$

Below, index "m" is always assumed to be equal to 0 and n_0 in the final expressions of the parameters used (especially when expressing integrals).

C. Solution for the coupling between the pressure field in the air gap and the pressure field inside the backchamber

The pressure variation $p_C(r)$ in the backchamber, solution of the propagation equation (7) and subjected to the Neumann boundary condition at $r = a$, takes the following form:

$$p_C(r,\theta) = -\frac{i\omega\rho_0}{\varepsilon_C F_{vC}}\sum_{mn}\frac{v_{mn}^2 J_m(\kappa_{mn}r)}{\kappa_{mn}^2-\chi_C^2} \times\left\{\left[U_1 J_m(\kappa_{mn}r_1)+U_m^{(1)}J_m(\kappa_{mn}r_2)\right]\cos(m\theta) + U_m^{(2)}J_m(\kappa_{mn}r_2)\sin(m\theta)\right\}, \tag{25}$$

which is the same kind of solution as solution (24b), the index "C" being associated with the thickness of the backchamber. Using Eqs. (9c) and (10e), namely

$$p(r_1,0) = p_C(r_1,0) - U_1/Y_1, \tag{26a}$$

$$p(r_2,\theta) = p_C(r_2,\theta) - U(\theta)/y, \tag{26b}$$

Eq. (25) leads to:

$$p(r_1,0) = -\left[\begin{array}{l}\left(\frac{1}{Y_1}+\frac{i\omega\rho_0}{\varepsilon_C F_{vC}}\sum_{mn}\frac{v_{mn}^2 J_m^2(\kappa_{mn}r_1)}{\kappa_{mn}^2-\chi_C^2}\right)U_1 \\ \quad +\frac{i\omega\rho_0}{\varepsilon_C F_{vC}}\sum_{mn}\frac{v_{mn}^2 J_m(\kappa_{mn}r_1)}{\kappa_{mn}^2-\chi_C^2}J_m(\kappa_{mn}r_2)\,U_m^{(1)}\end{array}\right], \tag{26c}$$

$$p(r_2,\theta) = -\frac{i\omega\rho_0}{\varepsilon_C F_{vC}}\sum_{mn}\frac{v_{mn}^2 J_m(\kappa_{mn}r_2)}{\kappa_{mn}^2-\chi_C^2} \times\left\{\cos(m\theta)\left[J_m(\kappa_{mn}r_1)\,U_1 + J_m(\kappa_{mn}r_2)\,U_m^{(1)}\right] + \sin(m\theta)J_m(\kappa_{mn}r_2)U_m^{(2)}\right\} - U(\theta)/y, \tag{26d}$$

namely, accounting for Eq. (22b),

$$p(r_2,\theta) = -\frac{i\omega\rho_0}{\varepsilon_C F_{vC}}\sum_{mn}\frac{v_{mn}^2 J_m(\kappa_{mn}r_2)}{\kappa_{mn}^2-\chi_C^2}J_m(\kappa_{mn}r_1)\,U_1\cos(m\theta) - \left[\frac{i\omega\rho_0}{\varepsilon_C F_{vC}}\sum_{mn}\frac{v_{mn}^2 J_m(\kappa_{mn}r_2)}{\kappa_{mn}^2-\chi_C^2}J_m(\kappa_{mn}r_1) + \frac{1}{\pi(1+\delta_{m0})y}\right]\left[U_m^{(1)}\cos(m\theta)+U_m^{(2)}\sin(m\theta)\right]. \tag{26e}$$

These equations can be written in the form of the following square matrix equation:

$$\begin{bmatrix} p(r_1,0) \\ p_0^{(1)}(r_2) \\ \ldots \\ p_m^{(1)}(r_2) \\ \ldots \end{bmatrix} = \begin{bmatrix} z_{hh} & z_{h0} & \ldots & z_{hm} & \ldots \\ z_{h0} & z_{s0} & 0 & 0 & 0 \\ \ldots & 0 & \ldots & 0 & 0 \\ z_{hm} & 0 & 0 & z_{sm} & 0 \\ \ldots & 0 & 0 & 0 & \ldots \end{bmatrix} \begin{bmatrix} U_1 \\ U_0^{(1)} \\ \ldots \\ U_m^{(1)} \\ \ldots \end{bmatrix}, \tag{27a}$$

$$\begin{bmatrix} p_1^{(2)}(r_2) \\ \\ p_m^{(2)}(r_2) \\ \\ \end{bmatrix} = \begin{bmatrix} z_{s1} & 0 & 0 & 0 \\ 0 & \ldots & 0 & 0 \\ 0 & 0 & z_{sm} & 0 \\ 0 & 0 & 0 & \ldots \end{bmatrix} \begin{bmatrix} U_1^{(2)} \\ \ldots \\ U_m^{(2)} \\ \ldots \end{bmatrix}, \tag{27b}$$

where

$$p_m^{(1)}(r_2) = \langle p(r_2,\theta)|\cos(m\theta)\rangle/[\pi\,(1+\delta_{m0})]$$
$$p_m^{(2)}(r_2) = \langle p(r_2,\theta)|\sin(m\theta)\rangle/[\pi\,(1+\delta_{m0})], \tag{27c}$$

and

$$z_{hh} = \left(-\frac{1}{Y_1}+\sum_m z_m(r_1,r_1)\right), \tag{27d}$$

$$z_{hm} = z_m(r_1, r_2), \tag{27e}$$

$$z_{sm} = -\frac{1}{\pi(1+\delta_{m0})y} + z_m(r_2, r_2), \tag{27f}$$

with

$$z_m(r_i, r_j) = -\frac{i\omega\rho_0}{\varepsilon_C F_{vC}} \sum_n \frac{v_{mn}^2 J_m(\kappa_{mn} r_i) J_m(\kappa_{mn} r_j)}{\kappa_{mn}^2 - \chi_C^2}. \tag{27g}$$

The unknowns considered here are, therefore, solutions of the linear set of algebraic equations where the matrix elements y_{ij} are known,

$$\begin{bmatrix} U_1 \\ U_0^{(1)} \\ \dots \\ U_m^{(1)} \\ \dots \end{bmatrix} = \begin{bmatrix} y_{hh} & y_{h0} & \dots & y_{hm} & \dots \\ y_{h0} & y_{00} & \dots & y_{0m} & \dots \\ \dots & \dots & \dots & \dots & \dots \\ y_{hm} & y_{0m} & \dots & y_{mm} & \dots \\ \dots & \dots & \dots & \dots & \dots \end{bmatrix} \begin{bmatrix} p(r_1, 0) \\ p_0^{(1)}(r_2) \\ \dots \\ p_m^{(1)}(r_2) \\ \dots \end{bmatrix}, \tag{28a}$$

$$\begin{bmatrix} U_1^{(2)} \\ \dots \\ U_m^{(2)} \\ \dots \end{bmatrix} = \begin{bmatrix} y_{s1} & 0 & 0 & 0 \\ 0 & \dots & 0 & 0 \\ 0 & 0 & y_{sm} & 0 \\ 0 & 0 & 0 & \dots \end{bmatrix} \begin{bmatrix} p_1^{(2)}(r_2) \\ \dots \\ p_m^{(2)}(r_2) \\ \dots \end{bmatrix}, \tag{28b}$$

with $y_{sm} = 1/z_{sm}$. Note that each matrix is symmetrical (even diagonal).

When considering only two modes "m" ($m = 0, 6$), Eq. (28a) takes the following form:

$$\begin{bmatrix} U_1 \\ U_0^{(1)} \\ U_6^{(1)} \end{bmatrix} = \frac{1}{z_{s0}z_{s6}z_{hh} - z_{h0}^2 z_{s6} + z_{h6}^2 z_{s0}} \times \begin{bmatrix} z_{s0}z_{s6} & -z_{h0}z_{s6} & -z_{s0}z_{h6} \\ -z_{h0}z_{s6} & z_{s6}z_{hh} - z_{h6}^2 & z_{h0}z_{h6} \\ -z_{s0}z_{h6} & z_{h0}z_{h6} & z_{s0}z_{hh} - z_{h0}^2 \end{bmatrix} \begin{bmatrix} p(r_1, 0) \\ p_0^{(1)}(r_2) \\ p_6^{(1)}(r_2) \end{bmatrix}. \tag{28c}$$

When using the microphone for classical applications (typically up to 20 kHz), the pressure variation p_C in the backchamber does not depend significantly on the azimuthal angle θ. In the lowest frequency range, this pressure variation is usually assumed to be uniform. These approximations are treated in Appendix A.

IV. THE DISPLACEMENT FIELD OF THE MEMBRANE

In this section, the following notations are used:

$$R_{\mu\nu} = T(K_{\mu\nu}^2 - K^2) - \frac{\rho_0\omega^2/(\varepsilon F_v)}{K_{\mu\nu}^2 - \chi^2}, \tag{29a}$$

$$\alpha_{\mu n} = \frac{-[\rho_0\omega^2/(\varepsilon F_v)]\, N_{\mu n}}{(K_{\mu n}^2 - \chi^2)} \frac{K_{\mu n} J'_\mu(K_{\mu n} a)}{\chi J'_\mu(\chi a)}, \tag{29b}$$

$$D_{\mu nq}^{(\sigma)} = \frac{i\omega\rho_0}{\varepsilon F_v} \frac{\pi[1 - (-)^\sigma \delta_{\mu 0}]}{R_{\mu n}} \frac{v_{\mu q}^2}{\kappa_{\mu q}^2 - \chi^2} \times \langle J_\mu(\kappa_{\mu q} r) | N_{\mu n} J_\mu(K_{\mu n} r) \rangle = \frac{i\omega\rho_0}{\varepsilon F_v} \frac{\pi[1 - (-)^\sigma \delta_{\mu 0}]}{R_{\mu n}} \frac{v_{\mu q}^2 N_{\mu n}}{\kappa_{\mu q}^2 - \chi^2} \times \frac{a K_{\mu n} J'_\mu(K_{\mu n} a) J_\mu(\kappa_{\mu q} a)}{\kappa_{\mu q}^2 - K_{\mu n}^2}, \tag{29c}$$

$$E_{0n} = \frac{2\pi}{R_{0n}} \frac{K_{0n}^2 - K^2}{K^2} \left\langle 1 - \frac{J_0(Kr)}{J_0(Ka)} \middle| N_{0n} J_0(K_{0n} r) \right\rangle \delta_{\mu 0} = \frac{2\pi}{R_{0n}} \frac{K_{0n}^2 - K^2}{K^2} N_{0n} \left[\frac{a}{K_{0n}} J_1(K_{0n} a) - \frac{a K_{0n} J'_0(K_{0n} a)}{K^2 - K_{0n}^2} \right] \delta_{\mu 0}, \tag{29d}$$

$$L_{\mu n}^{(\sigma)} = \frac{\pi[1 - (-)^\sigma \delta_{\mu 0}]}{R_{\mu n}} \langle J_\mu(\chi r) | N_{\mu n} J_\mu(K_{\mu n} r) \rangle = \frac{\pi[1 - (-)^\sigma \delta_{\mu 0}] N_{\mu n}}{R_{\mu n}} \frac{a K_{\mu n} J'_\mu(K_{\mu n} a) J_\mu(\chi a)}{\chi^2 - K_{\mu n}^2}, \tag{29e}$$

$$H_{\mu n}^{(I)} = y_{hh} J_\mu(\kappa_{\mu n} r_1) + y_{h\mu} J_\mu(\kappa_{\mu n} r_2), \tag{29f}$$

$$H_{\mu n\ell}^{(II)} = y_{h\ell} J_\mu(\kappa_{\mu n} r_1) + y_{\ell\mu} J_\mu(\kappa_{\mu n} r_2), \tag{29g}$$

$$H_{\mu n}^{(S)} = y_{s\mu} J_\mu(\kappa_{\mu n} r_2). \tag{29h}$$

A. Expression of the integration constant A_μ, Eq. (18c)

The inner product of the pressure variation $p(r, \theta)$ [Eqs. (15), (17), (18a), (18b), (23a), (28a), and (28b)] by the orthogonal eigenfunction $\psi_{\mu\nu}(r, \theta)$ [Eqs. (12a)–(12d)], invoking Eq. (18c) and notations mentioned above, is given by

$$\langle p(r, \theta) | N_{\mu\nu} J_\mu(K_{\mu\nu} r) \cos(\mu\theta) \rangle = R_{\mu\nu} L_{\mu\nu}^{(\sigma)} A_\mu^{(1)} + \frac{\rho_0\omega^2/(\varepsilon F_v)}{K_{\mu\nu}^2 - \chi^2} \xi_{\mu\nu}^{(1)} + R_{\mu\nu} \sum_n D_{\mu\nu n}^{(\sigma)} \times \left[H_{\mu n}^{(I)} p(r_1, 0) + \sum_{\ell=0, n_0, \dots} H_{\mu n\ell}^{(II)} p_\ell^{(1)}(r_2) \right], \tag{30a}$$

$$\langle p(r, \theta) | N_{\mu\nu} J_\mu(K_{\mu\nu} r) \sin(\mu\theta) \rangle = R_{\mu\nu} L_{\mu\nu}^{(\sigma)} A_\mu^{(2)} + \frac{\rho_0\omega^2/(\varepsilon F_v)}{K_{\mu\nu}^2 - \chi^2} \xi_{\mu\nu}^{(2)} + R_{\mu\nu} \sum_n D_{\mu\nu n}^{(\sigma)} H_{\mu n}^{(S)} p_\mu^{(2)}(r_2). \tag{30b}$$

Note that the left hand side of these equations can be written as

$$\langle p(r, \theta) | N_{\mu\nu} J_\mu(K_{\mu\nu} r) \cos(\mu\theta) \rangle = \pi(1 + \delta_{\mu 0}) \left\langle p_\mu^{(1)}(r) \middle| N_{\mu\nu} J_\mu(K_{\mu\nu} r) \right\rangle,$$

$$\langle p(r,\theta)\big|N_{\mu\nu}J_\mu(K_{\mu\nu}r)\sin(\mu\theta)\rangle = \pi(1-\delta_{\mu 0})\left\langle p_\mu^{(2)}(r)\middle|N_{\mu\nu}J_\mu(K_{\mu\nu}r)\right\rangle.$$

Invoking this last expression and the expression (18c) of the coefficients $A_m^{(\sigma)}$, and using the expression of the following inner products:

$$\langle 1\big|N_{\mu\nu}J_\mu(K_{\mu\nu}r)\cos(\mu\theta)\rangle = 2\pi\langle 1\big|N_{\mu\nu}J_\mu(K_{\mu\nu}r)\rangle\delta_{\mu 0},$$

$$\langle 1\big|N_{\mu\nu}J_\mu(K_{\mu\nu}r)\sin(\mu\theta)\rangle = 0,$$

Eq. (14b) takes the following form (using notations mentioned above):

$$\xi_{\mu\nu}^{(1)} = E_{0\nu}p_{av} + L_{\mu\nu}^{(1)}A_\mu^{(1)} + \sum_n D_{\mu\nu n}^{(1)}\left[H_{\mu n}^{(I)}p(r_1,0) + \sum_{\ell=0,n_0,\ldots} H_{\mu n\ell}^{(II)}p_\ell^{(1)}(r_2)\right], \tag{31a}$$

$$\xi_{\mu\nu}^{(2)} = L_{\mu\nu}^{(2)}A_\mu^{(2)} + \sum_n D_{\mu\nu n}^{(2)}H_{\mu n}^{(S)}p_\mu^{(2)}(r_2). \tag{31b}$$

Then, expression (18c) of A_μ takes the following form:

$$A_\mu^{(1)} = \frac{1}{1-\sum_q \alpha_{\mu q}L_{\mu q}^{(1)}}\sum_\nu \alpha_{\mu\nu}\left[p_{av}E_{0\nu} + \sum_n D_{\mu\nu n}^{(1)} \times\left(H_{\mu n}^{(I)}p(r_1,0) + \sum_{\ell=0,n_0,\ldots} H_{\mu n\ell}^{(II)}p_\ell^{(1)}(r_2)\right)\right], \tag{32a}$$

$$A_\mu^{(2)} = \frac{1}{1-\sum_q \alpha_{\mu q}L_{\mu q}^{(2)}}\sum_\nu \alpha_{\mu\nu}\sum_n D_{\mu\nu n}^{(2)}H_{\mu n}^{(S)}p_\mu^{(2)}(r_2). \tag{32b}$$

B. The pressure variation in the air gap and the displacement field of the membrane

The set of equations (31a), (31b) and (32a), (32b) leads straightforwardly to

$$\xi_{\mu\nu}^{(1)} = \Omega_{\mu\nu}^{(av)}p_{av} + \Omega_{\mu\nu}^{(h)}p(r_1,0) + \sum_{\ell=0,n_0,\ldots}\Omega_{\mu\nu\ell}^{(s1)}p_\ell^{(1)}(r_2), \tag{33a}$$

$$\xi_{\mu\nu}^{(2)} = \Omega_{\mu\nu}^{(s2)}p_\mu^{(2)}(r_2), \tag{33b}$$

with

$$\Omega_{\mu\nu}^{(av)} = E_{0\nu} + L_{\mu\nu}^{(1)}\frac{1}{1-\sum_q \alpha_{\mu q}L_{\mu q}^{(1)}}\sum_r \alpha_{\mu r}E_{0r}, \tag{33c}$$

$$\Omega_{\mu\nu}^{(h)} = L_{\mu\nu}^{(1)}\frac{1}{1-\sum_q \alpha_{\mu q}L_{\mu q}^{(1)}}\sum_r \alpha_{\mu r}\sum_n D_{\mu rn}^{(1)}H_{\mu n}^{(I)} + \sum_n D_{\mu\nu n}^{(1)}H_{\mu n}^{(I)}, \tag{33d}$$

$$\Omega_{\mu\nu\ell}^{(s1)} = L_{\mu\nu}^{(1)}\frac{1}{1-\sum_q \alpha_{\mu q}L_{\mu q}^{(1)}}\sum_r \alpha_{\mu r}\sum_n D_{\mu rn}^{(1)}H_{\mu n\ell}^{(II)} + \sum_n D_{\mu\nu n}^{(1)}H_{\mu n\ell}^{(II)}, \tag{33e}$$

$$\Omega_{\mu\nu}^{(s2)} = L_{\mu\nu}^{(2)}\frac{1}{1-\sum_q \alpha_{\mu q}L_{\mu q}^{(2)}}\sum_r \alpha_{\mu r}\sum_n D_{\mu rn}^{(2)}H_{\mu n}^{(S)} + \sum_n D_{\mu\nu n}^{(2)}H_{\mu n}^{(S)}. \tag{33f}$$

The pressure variation in the air gap [Eqs. (15), (17), (18a), (18b), (24b), (28a), and (28b)] is expressed as a function of the parameters p_{av}, $p(r_1,0)$, and $p_\ell^{(\sigma)}(r_2)$ when replacing $A_{mn}^{(\sigma)}$ and $\xi_{mn}^{(\sigma)}$ by their expression Eqs. (32a) and (32b) and (33a)–(33f), respectively,

$$p(r,\theta) = O_{av}(r,\theta)\,p_{av} + O_1(r,\theta)\,p(r_1,0) + \sum_{\sigma=1,2}\sum_{\ell=0,n_0,\ldots} O_{2\ell}^{(\sigma)}(r,\theta)\,p_\ell^{(\sigma)}(r_2), \tag{34a}$$

where

$$O_{av}(r,\theta) = \sum_{mn}\left[\frac{\alpha_{mn}E_{0n}}{1-\sum_q \alpha_{mq}L_{mq}^{(1)}}J_m(\chi r) + \frac{\rho_0\omega^2}{\varepsilon F_v}\frac{\Omega_{mn}^{(av)}N_{mn}}{K_{mn}^2-\chi^2}J_m(K_{mn}r)\right]\cos(m\theta), \tag{34b}$$

$$O_1(r,\theta) = \sum_{mn}\left[\frac{\alpha_{mn}\sum_t D_{mnt}^{(1)}H_{mt}^{(I)}}{1-\sum_q \alpha_{mq}L_{mq}^{(1)}}J_m(\chi r) + \frac{\rho_0\omega^2}{\varepsilon F_v}\frac{\Omega_{mn}^{(h)}N_{mn}}{K_{mn}^2-\chi^2}J_m(K_{mn}r) + \frac{i\omega\rho_0}{\varepsilon F_v}\frac{H_{mn}^{(I)}v_{mn}^2}{\kappa_{mn}^2-\chi^2}J_m(\kappa_{mn}r)\right]\cos(m\theta), \tag{34c}$$

$$O_{2\ell}^{(1)}(r,\theta) = \sum_{mn}\left[\frac{\alpha_{mn}\sum_t D_{mnt}^{(1)}H_{mt\ell}^{(II)}}{1-\sum_q \alpha_{mq}L_{mq}^{(1)}}J_m(\chi r) + \frac{\rho_0\omega^2}{\varepsilon F_v}\frac{\Omega_{mn\ell}^{(S1)}N_{mn}}{K_{mn}^2-\chi^2}J_m(K_{mn}r) + \frac{i\omega\rho_0}{\varepsilon F_v}\frac{H_{mn\ell}^{(II)}v_{mn}^2}{\kappa_{mn}^2-\chi^2}J_m(\kappa_{mn}r)\right]\cos(m\theta), \tag{34d}$$

$$O_{2m}^{(2)}(r,\theta) = \sum_{n}\left[\frac{\alpha_{mn}\sum_t D_{mnt}^{(2)}H_{mt}^{(S)}}{1-\sum_q \alpha_{mq}L_{mq}^{(2)}}J_m(\chi r) + \frac{\rho_0\omega^2}{\varepsilon F_v}\frac{\Omega_{mn}^{(S2)}N_{mn}}{K_{mn}^2-\chi^2}J_m(K_{mn}r) + \frac{i\omega\rho_0}{\varepsilon F_v}\frac{H_{mn}^{(S)}v_{mn}^2}{\kappa_{mn}^2-\chi^2}J_m(\kappa_{mn}r)\right]\sin(m\theta). \tag{34e}$$

TABLE I. Parameters of the B&K microphone type 4134 and air at 20 °C (Ref. 7).

Quantity	Symbols	Units	Value	Multiply by
Microphone size	—	in.	1/2 in.	—
Serial number	—	—	390329	—
Unpolarized capacitance	C	pF	17.4	—
Radius of the membrane	a	m	4.445	10^{-3}
Mass per unit area of the membrane	M_S	$\mathrm{kg\,m^{-2}}$	0.0445	—
Tension of the membrane	T	$\mathrm{N\,m^{-1}}$	3162.3	—
Density of air	ρ_0	$\mathrm{kg\,m^{-3}}$	1.20	—
Shear viscosity coefficient of air	μ	$\mathrm{kg\,m^{-1}\,s^{-3}}$	1.9	10^{-5}
Specific heat ratio	γ	—	1.403	—
Thickness of the fluid film (without polarization voltage)	ε	m	2.077	10^{-5}
Radius of the circular backing electrode	a_{bp}	m	3.607	10^{-3}
Number of holes in the backing electrode	n_0	—	6	—
Distance between the center of the backing electrode and the center of any hole	r_1	m	2.032	10^{-3}
Radius of the circular holes	R	m	5.080	10^{-4}
Length of the circular holes	h_1	m	0.843	10^{-3}
Distance between the center of the circular backing electrode and the peripheral slit	r_2	m	4.026	10^{-3}
Width of the peripheral slit	e	m	0.838	10^{-3}
Length of the peripheral slit	h_2	m	3.048	10^{-4}
Backchamber volume	V_C	$\mathrm{m^3}$	1.264	10^{-7}

Then, the parameters $p(r_1,0)$, and $p_\ell^{(\sigma)}(r_2)$ are expressed as functions of the incident pressure field p_{av} from the solution of the set of linear algebraic equations obtained first when writing expressions of $p(r,0)$ for $r=r_1$ and second when writing, for $r=r_2$, the inner product of $p(r,\theta)$, respectively, with $\cos(m\theta)$ and $\sin(m\theta)$.

Finally, the displacement field is expressed as a function of the incident pressure field p_{av} from Eqs. (14a) and (33a) and (33b), among the expressions of the parameters $p(r_1,\theta)$ and $p_\ell^{(\sigma)}(r_2)$. It is worth noting that the pressure field does not depend on the modes involving the function $\sin(\theta)$ when assuming that $m=0,6,\ldots$ because they vanish at the location of the holes.

V. RESULTS AND DISCUSSION

In this section, there are three major concerns regarding the use of electrostatic transducers. The first concern is the sensitivity of the microphone, which is a key parameter in most situations in the lower frequency range (up to 20 kHz), the second concern is the behavior of the displacement field of the membrane, which is of interest more particularly in the higher frequency range (up to 100 kHz), and the third concern is the mechanical-thermal noise, which can be evaluated from the mechanical resistance of the lumped element circuit (Appendix B). In order to compare the results obtained from the analytical modeling presented above with those available in the literature[7,25] and those given by the manufacturer, the microphone used here for both the analytical and the experimental studies is a Brüel & Kjær (B&K) pressure microphone type 4134. The values of the geometrical parameters of the microphone, the mechanical parameters of the membrane, and the thermo-acoustical parameters of the air used here are those given by Zuckerwar[7] (Table I).

In the experiment, the membrane of the microphone is driven by an electrostatic force creating an equivalent harmonic pressure field given by

$$p_{av}=\frac{C\,U_0}{\pi\,a^2\varepsilon}\,v, \tag{35}$$

where U_0 is the polarization voltage, and v is the time varying voltage (harmonic excitation).

A. Sensitivity

The sensitivity σ of the microphone is defined by the ratio of the open circuit output voltage and the incident pressure,

$$\sigma=-\frac{U_0}{\pi\,a^2 p_{av}}\sum_{m\,n\,\sigma}\xi_{mn}^{(\sigma)}\left\langle\psi_{mn}^{(\sigma)}(r,\,\theta)\right\rangle. \tag{36}$$

Herein, the calculated sensitivity assumes that the displacement field of the membrane and the pressure fields behind the membrane do not depend on the azimuthal angle θ ($m=0$, discarding higher order terms), while several values of the second integer n (labeling the zeros of the Neumann and Dirichlet eigenfunctions) are considered ($n=0$ to 10).

Figure 2 compares the sensitivity given on the B&K calibration chart with the results obtained from the analytical modeling. Two theoretical results are given for two values of the capacitance C, 17.4 and 16.0 pF (the relative difference between them being chosen to 8%) in order to show the effect on the sensitivity of the uncertainty on the thickness of the air gap. It appeared that the discrepancies between the experimental and analytical amplitudes cannot be interpreted by any uncertainties on the geometrical parameters. Nevertheless, these discrepancies could be explained partially when considering the real area of the backing electrode (lower than the area πa^2 of the membrane) in Eq. (35). This leads to a sensitivity of 9 mV/Pa, which is quite close to the experimental sensitivity 11 mV/Pa (to our knowledge, such analytical results were not available until now).

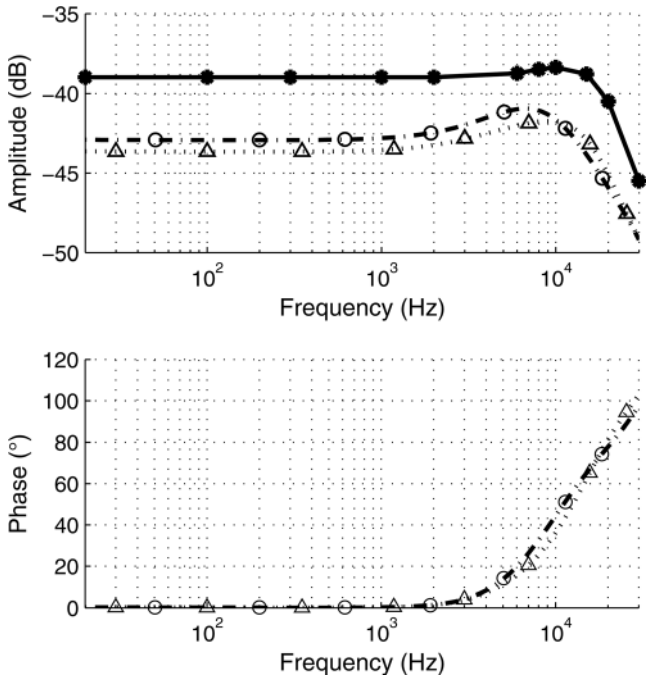

FIG. 2. Amplitude (dB re 1V/Pa) of the sensitivity, as a function of the frequency, as shown in the B&K calibration chart (solid line with stars), and amplitude and phase of the sensitivity calculated with two different values of the capacitance: $C = 17.4$ pF (dashed-dotted line with circles) and $C = 16$ pF (dotted line with triangles).

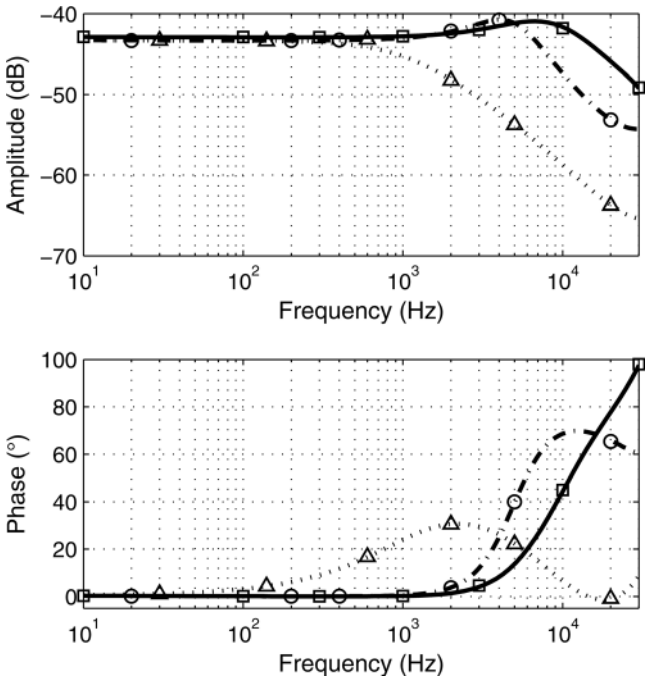

FIG. 3. Theoretical sensitivity as a function of the frequency. Solid line: Curve given in Fig. 2 (dashed-dotted line with circles) for $C = 17.4$ pF. Dashed-dotted line with circles and dotted line with triangles: Sensitivities obtained from the lumped element circuit presented in Appendix B, respectively, when using the exact values of the parameters and when using the lower order approximations.

Figure 3 compares the theoretical sensitivity as a function of the frequency for $C = 17.4$ pF given in Fig. 2 (dashed-dotted line with circles), shown in Fig. 3 (upper curve, solid line with squares), with the sensitivities obtained from the lumped element circuit presented in Appendix B, first when using the exact values of the parameters (dashed-dotted line with circles) and second when using the lower order approximations (dotted line with triangles) valid in the lower frequency range (up to 500 Hz). The behavior above roughly 2 kHz is due to the fact that the approximate model presented in Appendix B accounts for only one mode ($m = n = 0$).

B. Displacement field of the membrane

The displacement field of the membrane is obtained experimentally using a laser scanning vibrometer. It is calculated analytically using the procedure discussed in Sec. IV, accounting for the modes $m = 0$ and 6 only (with $n = 0$ to

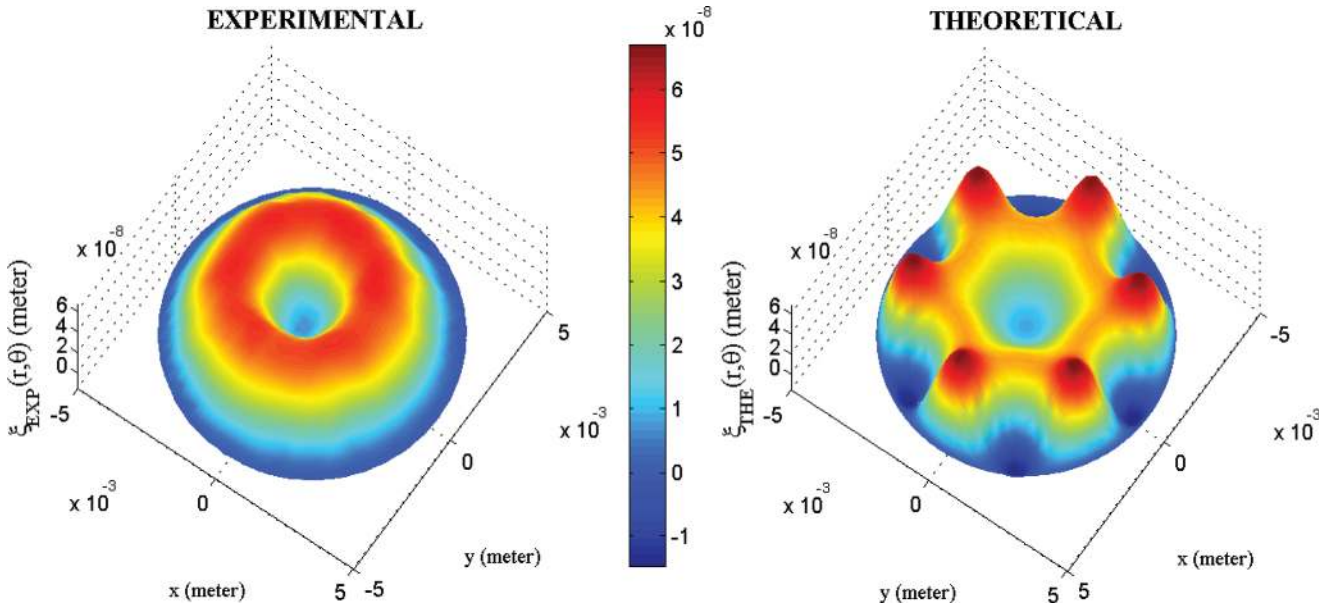

FIG. 4. (Color online) Measured (left) and calculated (right) displacement fields of the membrane of the B&K 4134 microphone at 40 kHz.

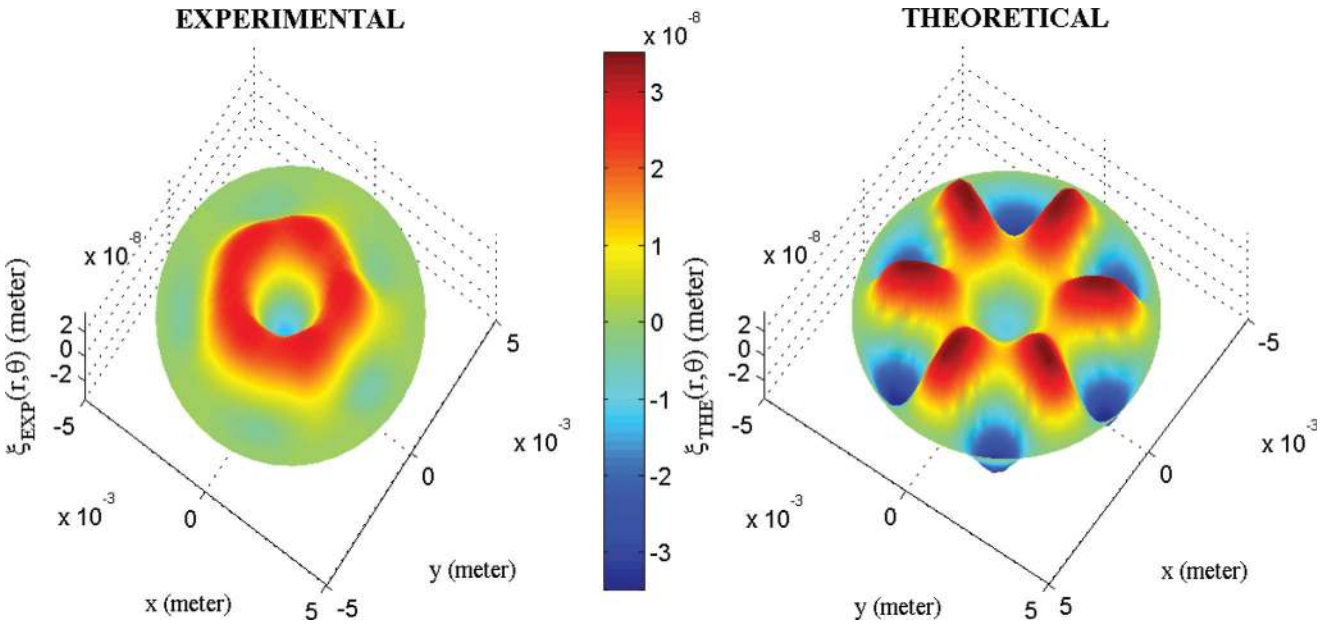

FIG. 5. (Color online) Measured (left) and calculated (right) displacement fields of the membrane of the B&K 4134 microphone at 70 kHz.

10) in order to emphasize the role played by the six holes in the backing electrode.

Two examples of theoretical and experimental displacement fields are given in Figs. 4 and 5, respectively, at 40 and 70 kHz, when the displacement reaches its maximum at the location of a hole. Experimental results show that the holes create a nonnegligible displacement of the membrane: At 40 kHz, they act in such a way that a ring appears at the radius of their location, and at 70 kHz, six bumps appear in front of their location.

Significant deviations between theoretical and experimental results appear. They may be due to the truncation of the number of modes considered here (the only azimuthal mode considered is the mode $m = 6$) and to the fact that the holes and the peripheral slit are modeled as Dirac sources (punctual sinks).

Nevertheless, these results give evidence of the accuracy of the model. Table II gives experimental and theoretical values of the displacement field magnitude at the location of the holes and at the center of the membrane, showing a quite good agreement between theoretical and experimental results. Comments on these results are given below in the conclusion (Sec. VI).

C. Mechanical resistance (thermal noise)

The mechanical-thermal noise can be evaluated from the mechanical resistance R_{th} of the lumped element circuit, which is defined by the real part of the total equivalent air impedance (Appendix B),

$$R_{th} = \Re(Z_g + Z_R). \tag{37}$$

The calculated equivalent resistance assumes that the displacement field of the membrane and the pressure fields behind the membrane are given at the lower order mode ($m = 0$, $n = 0$). This evaluation starts from the inner product (over the surface of the membrane) of eigenfunction ψ_{00} and the quantities of interest [Eq. (B8)] and leads to two values of the parameters of the lumped elements circuit (Fig. 7) for two orders of approximation [e.g., the parameter Z_Q is calculated from the two last expressions in Eq. (B28), which give, respectively, the first order and the zero order approximations].

Figure 6 gives the resistance R_{th} as a function of the frequency for the B&K microphone type 4134 when using the zero order approximation (solid line with triangles) and the first order approximation (dashed line with squares) for the parameters of the lumped element circuit. In the lower frequency range, the value obtained for the lower order approximation is 2.06×10^8 Ns/m^5 (corresponding to a mechanical-thermal noise equal to 20.2 dB[A]) and, for the first order approximation, it is 1.69×10^8 Ns/m^5. These results must be compared with those available in the literature (see for example Ref. 25, Table II) and more specifically with the value given by Zuckerwar, namely 1.89×10^8 Ns/m^5. As

TABLE II. Experimental and theoretical values of the displacement field magnitude in front of a hole and at the center of the membrane for 40 and 70 kHz.

Frequency (kHz)	Location	Experimental (nm)	Theoretical ($m = 0$ and 6) (nm)
40	In front of a hole	55.2	41.2
	At the center of the membrane	7.1	8.7
70	In front of a hole	35	30
	At the center of the membrane	−11	−8.3

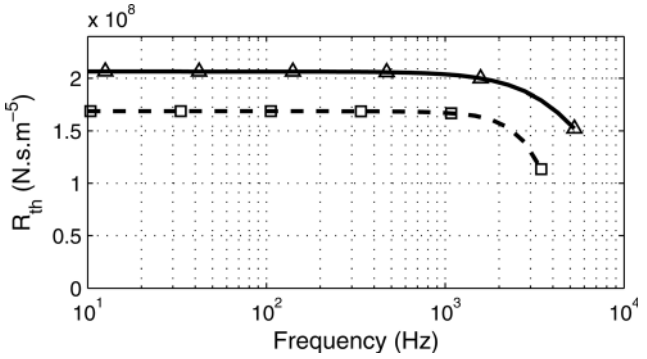

FIG. 6. Resistance R_{th} as a function of the frequency, when using the zero order approximation (solid line with triangles) and the first order approximation (dashed line with squares) for the parameters of the lumped element circuit B1.

expected, the result obtained for the first order approximation is more accurate; it is closer for the value obtained from the modified Škvor/Starr approach, which is much closer to the specification of 1.35×10^8 Ns/m^5 (corresponding to a mechanical-thermal noise equal to 18.3 dB[A]).

VI. CONCLUSIONS

The acoustic behavior of the membranes of electrostatic microphones (used either as receivers or as emitters) is important today because in several applications the coupling of these microphones with the acoustic field (generated or measured by them) must be known with very low uncertainties. Then, both experimental investigation and analytical modeling of the behavior of these membranes must provide results achieving a good accuracy.

The experimental results presented here, obtained from using a laser scanning vibrometer, provide quantitative information on the behavior of the displacement field of the membrane, in a broad frequency range (from 20 Hz to 80 kHz). More particularly, they show the large influence of the holes in the backing electrode on the membrane behavior for a large frequency range. Beside these experimental investigations, analytical results, which depart significantly from the current one, are presented.

The quite good agreement between the analytical and experimental results shows that the analytical solutions suggested here seem accurate enough to describe electrostatic microphones behavior (even other kind of transducers) in a huge frequency range and then are able to be used for the applications, which need accurate characterization of these transducers. Actually, owing to the approximations mentioned in the previous sections, several discrepancies appear between theoretical and experimental results. First, the amplitude and the width of the theoretical peaks of the displacement field of the membrane are sometimes, respectively, higher and smaller than the experimental peaks, and second, the theoretical sensitivity is slightly lower than the experimental sensitivity (given by the manufacturer). This is mainly due to the fact that the holes and the peripheral slit are modelized by Dirac sources (punctual sinks) and that the only azimuthal mode considered is the mode $m = 6$.

On this concern, to obtain more accurate results, the analytical model should be extended in such a way that the real surface of the holes and the slit be accounted for (assuming the same volume velocity at their input and at their output) and that the number of modes considered, both Dirichlet and Neumann ones, be much higher than those considered herein. Nevertheless, despite the remaining theoretical work to be done (which would be a straightforward extension of the model presented in this paper), several results given here, not available until now, may be useful for current applications (mentioned in the Introduction). But, thanks to the reductions assumed in the model used here, the theoretical results convey interpretations of the physical phenomena, namely the main features that govern the sensitivity and the direct influence of the holes on the deformation of the membrane, giving the role played by each part of the device. Then, requirements that have to be taken into account in the design of new such kind of transducers can be addressed, using the theoretical results obtained in this work.

It is worth noting that, while the modeling appears somewhat cumbersome, the numerical calculations are in fact simple and rapid to handle. This modeling would be effective in many applications even though the discrepancies between theoretical and experimental results, including the resonance frequencies, could be not negligible (this being mainly due to the uncertainties on the parameters of the microphones). Moreover, this work provides lumped element circuits more accurate than those currently used.

To conclude, it can be emphasized that, given the relative simplicity of the model used here to obtain the results (only two to four main modes, holes and slit assumed to be punctual), there is seen to be close agreement between analytical and experimental results, thereby supporting both the theoretical modeling and experimental measurements.

ACKNOWLEDGMENTS

The authors are indebted to Jean-Noël Durocher (Eng., Laboratoire National de métrologie et d'Essais) and to Nicolas Veau (Eng. Neurelec Society) for substantial help in organizing this account. They would like to express their thanks to Polytec GmbH society for helpful discussions on the metrology using the laser scanning vibrometer. This work has been funded by the Ministère de l'Enseignement Supérieur et de la Recherche, which has supported the research studentship of the first author when preparing his Ph.D. thesis that in part led to this paper.

APPENDIX A: PRESSURE VARIATION IN THE BACKCHAMBER, IN THE LOWER FREQUENCY RANGE

In the frequency range of interest, when using the microphone for classical applications (typically up to 20 kHz), the pressure variation p_C in the backchamber does not depend significantly on the azimuthal angle θ. Therefore, it can be written as follows:

$$p_C(r) = -\frac{i\omega\rho_0}{F_v\varepsilon_C}[U_1 G_C(r, r_1) + U_2 G_C(r, r_2)], \qquad \text{(A1)}$$

where $G_C(r, r_0)$ is the cylindrical Green's function satisfying Neumann boundary conditions given by

$$G_C(r, r_0) = \sum_n \frac{\varphi_{0n}(r_0)}{\kappa_{0n}^2 - \chi_C^2} \varphi_{0n}(r), \tag{A2}$$

the eigenfunctions $\varphi_{0n}(r)$ being given by

$$\varphi_{0n}(r) = v_{0n} J_m(\kappa_{0n} r). \tag{A3}$$

The pressure variations $p_C(r_1)$ and $p_C(r_2)$, respectively, at the location of the holes and the slit in the backchamber, are related to the volume velocities U_1 and U_2 by the following equations:

$$\begin{bmatrix} p_C(r_1) \\ p_C(r_2) \end{bmatrix} = -\frac{i\omega\rho_0}{F_v \varepsilon_C} \begin{bmatrix} G_C(r_1, r_1) & G_C(r_1, r_2) \\ G_C(r_2, r_1) & G_C(r_2, r_2) \end{bmatrix} \begin{bmatrix} U_1 \\ U_2 \end{bmatrix}. \tag{A4}$$

Therefore, the set of Eqs. (A4), (9c), and (10a) leads to the matrix equation

$$\begin{bmatrix} U_1 \\ U_2 \end{bmatrix} = \begin{bmatrix} y_{11} & y_{12} \\ y_{21} & y_{22} \end{bmatrix} \begin{bmatrix} p_1 \\ p_2 \end{bmatrix}, \tag{A5}$$

with

$$\begin{bmatrix} y_{11} & y_{12} \\ y_{21} & y_{22} \end{bmatrix} = \frac{\begin{bmatrix} -\varepsilon_C Y_1 Y_2 G_C(r_2, r_2) - [\varepsilon_C^2 F_v Y_1 / (i\omega\rho_0)] & \varepsilon_C Y_1 Y_2 G_C(r_1, r_2) \\ \varepsilon_C Y_1 Y_2 G_C(r_1, r_2) & -\varepsilon_C Y_1 Y_2 G_C(r_1, r_1) - [\varepsilon_C^2 F_v Y_2 / (i\omega\rho_0)] \end{bmatrix}}{i\omega\rho_0 (i\omega\rho_0 / F_v) [Y_1 Y_2 G_C(r_1, r_1) G_C(r_2, r_2) - Y_1 Y_2 G_C^2(r_1, r_2)] + \varepsilon_C [Y_1 G_C(r_1, r_1) + Y_2 G_C(r_2, r_2) + \varepsilon_C F_v / (i\omega\rho_0)]}. \tag{A6}$$

It is worth noting that the lower order term ($m = 0$) of these results given by

$$\kappa_{00} = 0\,,\ \varphi_{00} = \frac{1}{\sqrt{\pi}\, a}\,,\ G_C = -\frac{c_0^2}{\pi a^2 \omega^2} \tag{A7}$$

leads to the following expression for the pressure variation p_C (uniform inside the cavity):

$$p_C = -\frac{\rho_0 c_0^2}{i\omega V_C}(U_1 + U_2) = -\frac{\gamma P_0}{i\omega V_C}(U_1 + U_2), \tag{A8}$$

where $V_C \cong \pi a^2 \varepsilon_C$ is the volume of the backchamber, and P_0 is the static pressure. Thus, the ratio of the total volume velocity $(-U_1 - U_2)$ to the pressure variation p_C is the input admittance of a small cavity of volume V_C,

$$Y_C = \frac{1}{Z_C} = \frac{i\omega V_C}{\gamma P_0} = \frac{i\omega V_C\, \chi_T}{\gamma}, \tag{A9}$$

which is a good approximation in the lower frequency range.

Therefore, in the lower frequency range, Eq. (A6) can be written as

$$\begin{bmatrix} y_{11} & y_{12} \\ y_{21} & y_{22} \end{bmatrix} = \frac{1}{Y_1 + Y_2 + Y_C} \begin{bmatrix} -Y_1(Y_2 + Y_C) & Y_1 Y_2 \\ Y_1 Y_2 & -Y_2(Y_1 + Y_C) \end{bmatrix} \cong \begin{bmatrix} -Y_1 & Y_1 \\ Y_1 & -(Y_1 + Y_C) \end{bmatrix}, \tag{A10}$$

with $Y_2 = 2\pi y$ and where in the last expression the length of the slit is assumed to vanish (it is lower than both its thickness and the length of the holes).

APPENDIX B: LOWER ORDER APPROXIMATION

In this appendix, all the modes are neglected except the first one (0, 0), in order to obtain a mean input impedance of the microphone. The exact expressions and several expressions more or less approximated are provided for each parameter. The following notations are used:

$$\frac{1}{Z_g} = \frac{1}{Z_v} + \frac{1}{Z_h}, \tag{B1}$$

where

$$Z_v = \frac{i\omega\rho_0}{4\pi\varepsilon F_v}, \quad Z_h = \frac{-i\omega\rho_0 K_{00}^2}{4\pi\varepsilon F_v \chi^2}. \tag{B2}$$

Assuming that $(2 - \phi_r)/2 = 0.94 \cong 1$,

$$F_v = 1 - \frac{2 - \phi_r}{2} \frac{tg(k_v \varepsilon/2)}{k_v \varepsilon/2} \cong \frac{-1}{3} \left(k_v \frac{\varepsilon}{2}\right)^2 \left[1 + \frac{2}{5}\left(k_v \frac{\varepsilon}{2}\right)^2\right] = \left[\frac{12\,\mu}{i\omega\rho_0\varepsilon^2} + \frac{6}{5}\right]^{-1}, \tag{B3}$$

$$F_v\, \chi^2 = \frac{\omega^2}{c_0^2}[1 + (\gamma - 1)(1 - F_h)] = \frac{\omega^2}{c_0^2}\left[1 + (\gamma - 1)\frac{2 - \phi_r}{2}\frac{tg(k_h\varepsilon/2)}{k_h\varepsilon/2}\right] \cong \frac{\rho_0\, \chi_T\, \omega^2}{1 + i\omega\,(\gamma - 1/\gamma)(\rho_0 C_P \varepsilon^2 / 12\,\lambda_h)} = -i\omega\frac{\rho_0 K_{00}^2}{4\,\pi\,\varepsilon Z_h} \cong \gamma\frac{\omega^2}{c_0^2} = \rho_0\, \chi_T\, \omega^2, \tag{B4}$$

leading to

$$Z_v \cong R_\mu + i\omega L_\mu = \frac{12\,\mu}{4\pi\varepsilon^3} + i\omega\,\frac{1}{4\pi\varepsilon}\,\frac{6\rho_0}{5} \cong \frac{12\,\mu}{4\pi\varepsilon^3}, \tag{B5}$$

$$Z_h \cong R_h + \frac{1}{i\omega\,C_h} = \frac{K_{00}^2[(\gamma-1)/\gamma]\,\rho_0\,C_P\varepsilon}{4\pi\chi_T\,12\lambda_h} + \frac{1}{i\omega\,4\pi\varepsilon\chi_T/K_{00}^2} \cong \frac{1}{i\omega\,4\pi\varepsilon\chi_T/K_{00}^2}, \tag{B6}$$

and ($j_{00} = K_{00}a$)

$$Z_G = \left(\frac{2}{j_{00}}\right)^2 Z_g, \qquad Z_V = \left(\frac{2}{j_{00}}\right)^2 Z_v,$$
$$Z_H = \left(\frac{2}{j_{00}}\right)^2 Z_h \cong \frac{1}{i\omega\,\pi\,a^2\varepsilon\,\chi_T}, \tag{B7}$$

this last impedance representing the compressibility of the air gap. Note that the last expressions in the right hand side of Eqs. (B3)–(B7) provide approximations in the lowest frequency range.

Invoking Eqs. (15), (17), (18a), and (18b), the inner product (over the surface of the membrane) of Eq. (1a) and eigenfunction ψ_{00} leads straightforwardly to

$$\left[T\left(K_{00}^2 - K^2\right) + Q_{00}\,2\pi\langle\psi_{00}(r)|J_0(\chi r)\rangle - \frac{\rho_0\omega^2/\varepsilon F_v}{K_{00}^2-\chi^2} - 2\pi\langle\psi_{00}(r)|\Pi_{00}\rangle\right]\xi_{00} = -p_{av}2\pi\langle\psi_{00}(r)\rangle. \tag{B8}$$

Invoking (18c) and (24b), accounting for that $J_0(\kappa_{00}r) = 1$,

$$\begin{aligned} Q_{00} &= \frac{\rho_0\omega^2}{\varepsilon F_v}\,\frac{N_{00}}{K_{00}^2-\chi^2}\,\frac{K_{00}J_0'(K_{00}a)}{\chi J_0'(\chi a)} \\ &= \frac{\rho_0\omega^2}{K_{00}^2}\,\frac{K_{00}^2/(\varepsilon F_v)}{K_{00}^2-\chi^2}\,\frac{1/(\sqrt{\pi}\,a)}{J_1(K_{00}a)}\,\frac{K_{00}J_0'(K_{00}a)}{\chi J_0'(\chi a)} \\ &\cong i\omega\,\frac{2\sqrt{\pi}}{K_{00}}\,\frac{Z_h}{Z_v}Z_G\,\frac{1}{1-(1/2)\,(\chi a/2)^2} \\ &= i\omega\,\frac{2\sqrt{\pi}}{K_{00}}\,\frac{Z_h}{Z_v}Z_G\,\frac{1}{1+(1/2)\,Z_v/Z_H}, \end{aligned} \tag{B9}$$

$$\psi_{00}(r) = \frac{J_0(K_{00}r)}{\sqrt{\pi}\,a\,J_1(K_{00}a)} \cong \frac{1-(K_{00}\,r/2)^2}{\pi\,a^2\,K_{00}\Big/(2\sqrt{\pi})\left[1-(1/2)(K_{00}a/2)^2\right]}, \tag{B10}$$

$$2\pi\langle\psi_{00}(r)\rangle = \frac{2\sqrt{\pi}}{K_{00}}, \tag{B11}$$

$$\begin{aligned} 2\pi\langle\psi_{00}|J_0(\chi r)\rangle &= \frac{2\sqrt{\pi}}{a\,J_1(K_{00}a)}\,\frac{K_{00}aJ_1(K_{00}a)J_0(\chi a)}{2\left(K_{00}^2-\chi^2\right)} \\ &= \frac{2\sqrt{\pi}K_{00}}{\left(K_{00}^2-\chi^2\right)}\,J_0(\chi a) \\ &\cong \frac{2\sqrt{\pi}}{K_{00}}\,\frac{K_{00}^2}{\left(K_{00}^2-\chi^2\right)}\left[1-\left(\frac{\chi a}{2}\right)^2\right] \\ &= \frac{2\sqrt{\pi}}{K_{00}}\frac{Z_g}{Z_v}\left[1+\frac{Z_v}{Z_H}\right], \end{aligned} \tag{B12}$$

$$\Pi_{00} = \Pi_{00}\,J_0(\kappa_{00}r) = p_u(r)/\xi_{00}. \tag{B13}$$

It is worth noting that the "effective" area of the membrane is given by

$$\left(\frac{2\sqrt{\pi}}{K_{00}}\right)^2 = \frac{\pi a^2}{(K_{00}a/2)^2} \cong \frac{\pi a^2}{(j_{00}/2)^2} \cong 0.7\pi a^2. \tag{B14}$$

The parameter $\Pi_{00} = p_u(r)/\xi_{00}$ can be expressed as follows (24b):

$$\Pi_{00} = \frac{\sigma_{00}}{\xi_{00}}\left\{H_{00}^{(I)}\,p(r_1) + H_{00}^{(II)}\,p(a)\right\}, \tag{B15}$$

with, invoking Eq. (A10),

$$\begin{aligned} \sigma_{00} &= \frac{i\omega\rho_0}{\varepsilon F_v}\,\frac{v_{00}^2}{\kappa_{00}^2-\chi^2} = \frac{i\omega\rho_0/F_v}{\pi a^2\left(\kappa_{00}^2-\chi^2\right)} \\ &= \frac{-i\omega\rho_0}{\pi a^2\varepsilon F_v\chi^2} = \left(\frac{2}{K_{00}a}\right)^2 Z_h = Z_H, \end{aligned} \tag{B16}$$

$$\begin{aligned} H_{00}^{(I)} &= y_{hh}J_0(\kappa_{00}r_1) + y_{h0}J_0(\kappa_{00}a) = y_{hh} + y_{h0} \\ &= -\frac{Y_CY_1}{Y_C+Y_1+Y_2}, \end{aligned} \tag{B17}$$

$$\begin{aligned} H_{00}^{(II)} &= y_{h0}J_0(\kappa_{00}r_1) + y_{00}J_0(\kappa_{00}a) = y_{h0} + y_{00} \\ &= -\frac{Y_CY_2}{Y_C+Y_1+Y_2}. \end{aligned} \tag{B18}$$

Invoking the following expression of $p(r)$ (Sec. III B):

$$\frac{p(r)}{\xi_{00}} = -Q_{00}J_0(\chi r) + \frac{\rho_0\omega^2/\varepsilon F_v}{K_{00}^2-\chi^2}\psi_{00}(r) + \Pi_{00}, \tag{B19}$$

Eq. (B15) can be written as

$$\Pi_{00} = \sigma_{00}\left\{H_{00}^{(I)}\left[F_{00}^{(1)}(r_1) + \Pi_{00}\right] + H_{00}^{(II)}\left[F_{00}^{(2)}(r_2) + \Pi_{00}\right]\right\}, \tag{B20}$$

where ($r_2 \cong a$)

$$\begin{aligned} F_{00}^{(i)}(r_i) &= -Q_{00}\,J_0(\chi r_i) + \frac{\rho_0\omega^2/(\varepsilon F_v)}{K_{00}^2-\chi^2}\psi_{00}(r_i) \\ &\cong -i\omega\frac{2\sqrt{\pi}}{K_{00}}\left[\frac{Z_h}{Z_v}Z_G\,\frac{J_0(\chi r_i)}{1+(1/2)Z_v/Z_H} + \frac{2\sqrt{\pi}}{K_{00}}Z_g\,\frac{J_0(K_{00}r_i)}{\sqrt{\pi}aJ_1(K_{00}a)}\right] \\ &\cong -i\omega\frac{2\sqrt{\pi}}{K_{00}}\,Z_G\left[\frac{Z_h}{Z_v}\frac{1+(K_{00}r_i/2)^2(Z_v/Z_h)}{1+(1/2)Z_v/Z_H} + \frac{1-(K_{00}r_i/2)^2}{1-(1/2)(K_{00}a/2)^2}\right] \\ &\cong -i\omega\frac{2\sqrt{\pi}}{K_{00}}Z_G\left[\frac{Z_h}{Z_v}+1-\frac{1}{2}\left(\frac{K_{00}r_i}{2}\right)^2\frac{Z_v}{Z_H}\right] \\ &\cong -i\omega\frac{2\sqrt{\pi}}{K_{00}}Z_G\frac{Z_H}{Z_G} = -i\omega\frac{2\sqrt{\pi}}{K_{00}}Z_H, \end{aligned} \tag{B21}$$

leading to

$$\Pi_{00} = \frac{H_{00}^{(I)} F_{00}^{(1)} + H_{00}^{(II)} F_{00}^{(2)}}{(1/\sigma_{00}) - \left(H_{00}^{(1)} + H_{00}^{(2)}\right)} = \frac{H_{00}^{(I)} F_{00}^{(1)} + H_{00}^{(II)} F_{00}^{(2)}}{1/Z_H + 1/Z_B}, \tag{B22a}$$

with

$$Z_B = Z_C + \frac{Z_1 Z_2}{(Z_1 + Z_2)}, \tag{B22b}$$

Z_1, Z_2, and Z_C being given by Eqs. (9b), (10b), and (A9), respectively, their approximate expressions being given by

$$Z_1 = \frac{1}{n_0 y_1} \cong \frac{1}{n_0}\left(\frac{8\,\mu\,h_1}{\pi R^4} + i\omega\,\frac{(4\rho_0/3)\,h_1}{\pi R^2}\right) \cong \frac{1}{n_0}\frac{8\,\mu\,h_1}{\pi R^4}, \tag{B23a}$$

$$Z_2 \cong \frac{12\,\mu\,h_2}{2\,\pi\,a\,e^3} + i\omega\,\frac{(6\rho_0/5)\,h_2}{2\,\pi\,a\,e} \cong \frac{12\,\mu\,h_2}{2\,\pi\,a\,e^3}, \tag{B23b}$$

$$Z_C \cong \frac{1}{i\omega\,C_C} \cong \frac{\gamma}{i\omega\,V_C\,\chi_T}. \tag{B23c}$$

Finally, the input impedance of the microphone

$$Z_{av} = \frac{-p_{av}}{i\omega\,\xi_{00}\langle\psi_{00}(r)\rangle} = \frac{1}{i\omega}\left(\frac{K_{00}}{2\sqrt{\pi}}\right)^2\left(\frac{-p_{av}2\,\pi\langle\psi_{00}(r)\rangle}{\xi_{00}}\right) = \frac{1}{i\omega}\left(\frac{K_{00}}{2\sqrt{\pi}}\right)^2\left[T\left(K_{00}^2 - K^2\right) - \frac{\rho_0\omega^2/\varepsilon F_v}{K_{00}^2 - \chi^2} + Q_{00}\,2\,\pi\langle\psi_{00}(r)|J_0(\chi r)\rangle - 2\,\pi\langle\psi_{00}(r)|\Pi_{00}\rangle\right], \tag{B24}$$

can be expressed as

$$Z_{av} = Z_m + Z_g + Z_R, \tag{B25a}$$

with

$$Z_R = Z_Q + Z_P, \tag{B25b}$$

where

$$Z_m = \frac{1}{i\omega}\left(\frac{K_{00}}{2\sqrt{\pi}}\right)^2 T\left(K_{00}^2 - K^2\right) \cong i\omega L_m + \frac{1}{i\omega C_m}, \tag{B26a}$$

with

$$L_m = \frac{K_{00}^2}{4\pi} M_S, \qquad C_m = \frac{4\pi}{K_{00}^4}\frac{1}{T}, \tag{B26b}$$

$$Z_g = \frac{1}{i\omega}\left(\frac{K_{00}}{2\sqrt{\pi}}\right)^2\left[-\frac{\rho_0\omega^2/(\varepsilon F_v)}{K_{00}^2 - \chi^2}\right] \cong 1\Big/\left[\frac{1}{R_\mu + i\omega L_\mu} + \frac{1}{R_h + 1/(i\omega\,C_h)}\right], \tag{B27a}$$

with

$$R_\mu = \frac{12\mu}{4\pi\varepsilon^3}, \quad L_\mu = \frac{1}{4\pi\varepsilon}\frac{6\rho_0}{5}, \quad R_h = \frac{K_{00}^2[(\gamma-1)/\gamma]\rho_0 C_P \varepsilon}{4\pi\chi_T 12\lambda_h}, \quad C_h = \frac{4\pi\varepsilon}{K_{00}^2}\chi_T, \tag{B27b}$$

$$Z_Q = \frac{1}{i\omega}\left(\frac{K_{00}}{2\sqrt{\pi}}\right)^2 Q_{00} 2\pi\langle\psi_{00}(r)|J_0(\chi r)\rangle = \left(\frac{Z_g}{Z_v}\right)^2 Z_H\left[1 + \frac{1}{2}\frac{Z_v}{Z_H}\right] \cong Z_H, \tag{B28}$$

$$Z_P = \frac{-1}{i\omega}\left(\frac{K_{00}}{2\sqrt{\pi}}\right)^2 2\pi\langle\psi_{00}(r)|\Pi_{00}\rangle = \frac{1}{i\omega}\frac{K_{00}}{2\sqrt{\pi}}(-\Pi_{00}) \cong \frac{-Z_H}{1 + Z_B/Z_H}, \tag{B29}$$

Z_R taking then the following form to the lower order approximation:

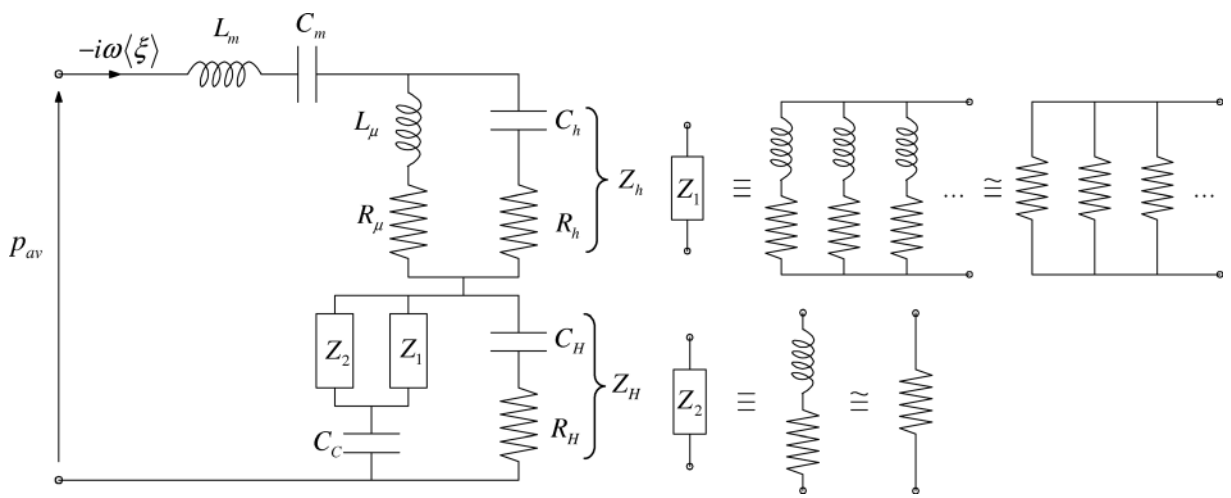

FIG. 7. Equivalent network of the input acoustic impedance [Eqs. (B22)–(B30)].

$$Z_R \cong Z_H - \frac{Z_H}{1+Z_B/Z_H} = \frac{Z_B}{1+Z_B/Z_H} = \frac{Z_B Z_H}{Z_B+Z_H}. \quad \text{(B30)}$$

It is worth noting that

$$\text{when } Z_B \to 0, \quad Z_R \to 0 \text{ (open air gap)}, \quad \text{(B31)}$$

$$\text{when } Z_B \to \infty, \quad Z_R \to Z_H \text{ (closed air gap)}. \quad \text{(B32)}$$

An equivalent network (lumped element circuit) of the input acoustic impedance [Eqs. (B25)–(B30)] is shown in Fig. 7. The relative complexity of this impedance Z_{av} emphasizes the complex behavior of the acoustic field behind the membrane. The equivalent network enlightens the role played by the main structures of the device, mainly through the impedances Z_m, Z_g, Z_R, and Z_B included in Z_{av}. Note that Fig. 7 corresponds to Eqs. (B22)–(B30).

APPENDIX C: EQUATIONS GOVERNING THE PRESSURE AND TEMPERATURE VARIATIONS IN THE AIR GAP

The fundamental linear equations which give an accurate description of the small amplitude disturbances inside the viscous and thermal boundary layers must satisfy several assumptions in order to avoid overly intricate formulations.

First, as the wavelength is much greater than the thickness of the air gap, the pressure variation p can be assumed constant over this thickness, and the z-component of the particle velocity v_z can be assumed much lower than its component v_r parallel to the electrodes (that is the flow is assumed to be essentially tangential to the membrane and the backing electrode). Therefore, in a first approximation, the Navier–Stokes equation is substituted by the Hagen–Poiseuille equation for the v_r-component tangent to the walls (the z-component of the particle velocity being nevertheless accounted for in the conservation of mass equation to assume the volume flow conservation).

Second, the spatial variations in the z-direction normal to the electrodes of both the r component v_r of the particle velocity and the temperature variation τ are much greater than the spatial variations in the tangential directions. Hence, the spatial variations of these quantities in the tangential direction can be neglected in the Navier–Stokes equation and in the Fourier heat conduction equation, respectively.

Therefore, the complete set of fundamental equations and boundary conditions governing the fluid motion inside the fluid gap, involving these approximations, is straightforwardly obtained, leading to, for harmonic perturbations (see Ref. 23, Chap. 3):

(i) for the r-component v_r of the particle velocity,

$$\left(\partial_{zz}^2 + k_v^2\right) v_r(r,z) = -\frac{k_v^2}{i\omega\rho_0}\partial_r p(r), \forall z \in (0,-\varepsilon), \quad \text{(C1a)}$$

with (2b)

$$v_r(r,0) = 0, \quad \text{(C1b)}$$

$$v_r(r,-\varepsilon) \cong \left[\frac{-\phi_r}{i\omega\rho_0}\right]\partial_r p(r), \quad \text{(C1c)}$$

the Euler equation being given by $v_r \cong [-1/(i\omega\rho_0)]\partial_r p$.

(ii) for the temperature variation τ (Fourier equation where the entropy variation is expressed from the pressure variations and the temperature variations),

$$\left(\partial_{zz}^2 + k_h^2\right)\tau(r,z) = k_h^2 \frac{\gamma-1}{\hat{\beta}\gamma} p(r), \forall z \in (0,-\varepsilon), \quad \text{(C2a)}$$

with

$$\tau(r,0) = 0, \quad \text{(C2b)}$$

$$\tau(r,-\varepsilon) \cong \phi_r \left[\frac{(\gamma-1)}{\hat{\beta}\gamma}\right] p(r), \quad \text{(C2c)}$$

the adiabatic law being given by $\tau \cong [(\gamma-1)/(\hat{\beta}\gamma)]p$.

The solutions[11] for both the r-component of the particle velocity and the temperature variation can be expressed as the sum of a particular solution of the propagation equations (C1a), and (C2a) with the uniform (i.e., non-z-dependent) term in the right hand side, namely,

$$\frac{-\partial_r p}{i\omega\rho_0} \quad \text{(C3a)}$$

for v_r [Eq. (C1a)] and

$$\left[\frac{(\gamma-1)}{\hat{\beta}\gamma}\right] p \quad \text{(C3b)}$$

for τ [Eq. (C2a)], and the general solution of the associated homogeneous equations (when the right hand side is substituted to zero), i.e., respectively,

$$A_v \cos k_v(z+\varepsilon/2) + B_v \sin k_v(z+\varepsilon/2), \quad \text{(C4a)}$$

$$A_h \cos k_h(z+\varepsilon/2) + B_h \sin k_h(z+\varepsilon/2). \quad \text{(C4b)}$$

Then the solutions of Eqs. (C1a) and (C2a), subject, respectively, to the boundary conditions (C1b) and (C1c) and Eqs. (C2b) and (C2c) are given by[11]

$$v_r(r,z) = -\frac{\partial_r p(r)}{i\omega\rho_0}\left[1 - \frac{2-\phi_r}{2}\frac{\cos k_v(z+\varepsilon/2)}{\cos k_v\varepsilon/2} - \frac{\phi_r}{2}\frac{\sin k_v(z+\varepsilon/2)}{\sin k_v\varepsilon/2}\right], \quad \text{(C5)}$$

$$\tau(r,z) = \frac{(\gamma-1)}{\hat{\beta}\gamma} p(r)\left[1 - \frac{2-\phi_r}{2}\frac{\cos k_h(z+\varepsilon/2)}{\cos k_h\varepsilon/2} - \frac{\phi_r}{2}\frac{\sin k_h(z+\varepsilon/2)}{\sin k_h\varepsilon/2}\right]. \quad \text{(C6)}$$

These results lead straightforwardly to the mean values $\bar{v}_r$ of the radial velocity v_r and $\bar{\tau}$ of the temperature variation τ across the thickness of the air gap [Eqs. (4) and (5), respectively].

It is worth noting that the expression (8c) comes from the same discussion as the one presented above, where variables r and z are permuted (function tan = sin/cos being replaced by J_1/J_0) and where $\phi_r = 0$.

Finally, eliminating the variables r and τ in the set of the three fundamental equations, namely Eqs. (C5), (C6), and equation of mass conservation (accounting for the usual expression of the density ρ as a function of p and τ), yields the propagation equation (6a).

[1]D. H. Robey, "Theory of the effect of a thin air film on the vibrations of a stretched circular membrane," J. Acoust. Soc. Am. **26**, 740–745 (1954).
[2]I. G. Petritskaya, "Impedance of a thin layer of air in the harmonic vibration of membrane," Sov. Phys. Acoust. **12**, 193–198 (1966).
[3]I. G. Petritskaya, "Vibrations of membrane loaded with thin layer of air," Sov. Phys. Acoust. **14**, 105–106 (1968).
[4]Z. Škvor, "On acoustical resistance due to viscous losses in the air gap of electrostatic transducers," Acustica **19**, 295–297 (1968).
[5]J. E. Warren, A. M. Brzezinski, and J. F. Hamilton, "Capacitance microphone dynamic membrane deflections," J. Acoust. Soc. Am. **54**(5), 1201–1213 (1973).
[6]J. E. Warren, "Capacitance microphone static membrane deflections: Comments and further results," J. Acoust. Soc. Am. **58**(3), 1201–1213 (1975).
[7]A. J. Zuckerwar, "Theoretical response of condenser microphones," J. Acoust. Soc. Am. **64**(5), 1278–1285 (1978).
[8]C. W. Tan and J. M. Miao, "Analytical modeling for bulk-micromachined condenser microphones," J. Acoust. Soc. Am. **120**(2), 750–761 (2006).
[9]D. Homentcovshi and R. N. Miles, "Modelling of viscous damping of perforated planar microstructures. Applications in acoustics," J. Acoust. Soc. Am. **116**(5), 2939–2947 (2004).
[10]D. Homentcovshi and R. N. Miles, "Viscous microstructural dampers with aligned holes: Design procedure including the edge correction," J. Acoust. Soc. Am. **112**(3), 1556–1567 (2007).
[11]R. S. Grinnip, "*Advance Simulation of a Condenser Microphone Capsule*," in AES 117th Convention, San Francisco (2004).
[12]M. Bruneau, A.-M. Bruneau, Z. Škvor, and P. Lotton, "An equivalent network modelling the strong coupling between a vibrating membrane and a fluid film," Acta Acoust. **2**, 223–232 (1994).
[13]T. Le Van Suu, S. Durand, and M. Bruneau, "Fluid layer trapped between a plane, circular membrane and an axisymmetrically curved, smooth backing wall: Analytical model of the dynamic behaviour," Acta Acust. **94**(3), 474–482 (2008).
[14]P. Honzík, Z. Škvor, S. Durand, and M. Bruneau, "Theoretical investigation on electrostatic transducers with non-planar backing electrode," Acta Acust. **95**(5), 671–686 (2009).
[15]W. G. Thomas, M. J. Preslar, and J. C. Farmer, "Calibration of condenser microphones under increased atmospheric pressures," J. Acoust. Soc. Am. **51**, 6–14 (1972).
[16]K. Rasmussen, "The static pressure and temperature coefficients of laboratory standard microphones," Metrologia **36**, 265–273 (1999).
[17]C. Guianvarc'h, R. Gavioso, G. Benedetto, L. Pitre, and M. Bruneau, "Characterization of condenser microphones under different environmental conditions for accurate speed of sound measurements with acoustic resonators," Rev. Sci. Instrum. **80**(7), 1–10 (2009).
[18]International Electrotechnical Commission, IEC61094-6: *Measurement Microphones, Part 6: Electrostatic Actuators for Determination of Frequency Response* (2004), http://webstore.iec.ch/webstore/webstore.nsf/ Artnum_PK/33395.
[19]C. Guianvarc'h, J.-N. Durocher, M. Bruneau, and A.-M. Bruneau, "Improved formulation of the acoustic transfer admittance of cylindrical cavities," Acta Acust. **92**, 345–354 (2006).
[20]J. B. Mehl, M. R. Moldover, and L. Pitre, "Designing quasi-spherical resonator for acoustic thermometry," Metrologia **41**, 295–304 (2004).
[21]G. Behler and M. Vorländer, "Reciprocal measurements on condenser microphones for quality control and absolute calibration," Acta Acust **90**, 152–160 (2004).
[22]S. Barrera-Figueroa, K. Rasmussen, and F. Jacobsen, "Radiation impedance of condenser microphones and their diffuse-field responses," J. Acoust. Soc. Am. **127**(4), 2290–2294 (2010).
[23]M. Bruneau and T. Scelo (translator and contributor), *Fundamentals of Acoustics* (ISTE, London, 2006).
[24]D. Rodrigues, C. Guianvarc'h, J.-N. Durocher, M. Bruneau, and A.-M. Bruneau, "A method to measure and interpret input impedance of small acoustic components," J. Sound Vib. **315**(4–5), 890–910 (2008).
[25]C. W. Tan and J. M. Miao, "Modified Škvor/Starr approach in the mechanical-thermal noise analysis of condenser microphone," J. Acoust. Soc. Am. **126**(5), 2301–2305 (2009).